Helsinki University of Technology
Materials Physics Laboratory
Espoo 2004

VORTICES AND ELEMENTARY EXCITATIONS IN DILUTE BOSE-EINSTEIN CONDENSATES

Mikko Möttönen

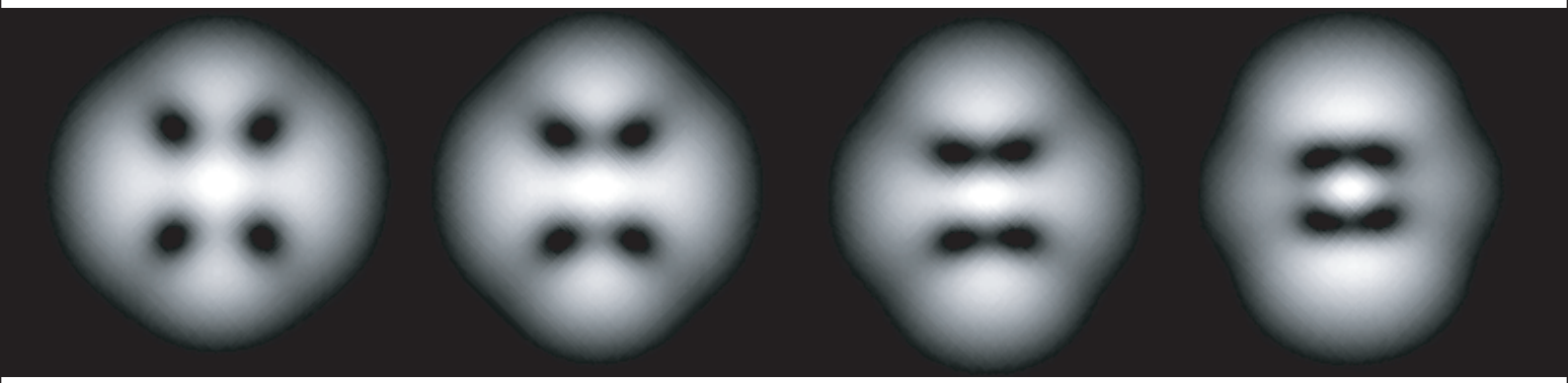

TEKNILLINEN KORKEAKOULU
TEKNISKA HÖGSKOLAN
HELSINKI UNIVERSITY OF TECHNOLOGY
TECHNISCHE UNIVERSITÄT HELSINKI
UNIVERSITE DE TECHNOLOGIE D'HELSINKI

Helsinki University of Technology Publications in Engineering Physics

Teknillisen korkeakoulun teknillisen fysiikan julkaisuja

Espoo 2004 TKK-F-A835

VORTICES AND ELEMENTARY EXCITATIONS IN DILUTE BOSE-EINSTEIN CONDENSATES

Mikko Möttönen

Dissertation for the degree of Doctor of Technology to be presented with due permission of the Department of Engineering Physics and Mathematics for public examination and debate in Auditorium F1 at Helsinki University of Technology (Espoo, Finland) on the 27th of December, 2004, at 14 o'clock.

Helsinki University of Technology
Department of Engineering Physics and Mathematics
Materials Physics Laboratory

Teknillinen korkeakoulu
Teknillisen fysiikan ja matematiikan osasto
Materiaalifysiikan laboratorio

Distribution:
Helsinki University of Technology
Materials Physics Laboratory
P.O. Box 2200
FIN-02015 HUT
Tel. +358-9-451-2342
Fax. +358-9-451-3164
E-mail: mikko.mottonen@hut.fi

ISBN 951-22-7439-6 (printed)
ISBN 951-22-7440-X (pdf)
ISSN 1456-3320

PicaSet Oy
Helsinki 2004

HELSINKI UNIVERSITY OF TECHNOLOGY
P.O. BOX 1000, FIN-02015 HUT
http://www.hut.fi

ABSTRACT OF DOCTORAL DISSERTATION

Author Mikko Möttönen

Name of the dissertation

VORTICES AND ELEMENTARY EXCITATIONS IN DILUTE BOSE-EINSTEIN CONDENSATES

Date of manuscript 16.11.2004 | Date of the dissertation 27.12.2004

☐ Monograph ☑ Article dissertation (summary + original articles)

Department Department of Engineering Physics and Mathematics
Laboratory Materials Physics Laboratory
Field of research Bose-Einstein condensates
Opponent(s) Professor Henrik Smith
Supervisor Professor Martti M. Salomaa
(Instructor) Dr. Tech. Sami M. M. Virtanen

Abstract

The condensation of weakly interacting alkali atom gases observed in 1995 is a manifestation of the macroscopic quantum phenomenon called Bose-Einstein condensation. In contrast to superconductivity and Helium superfluids, the dilute alkali atom condensates are directly observable using optical imaging techniques and they constitute highly controllable quantum systems. Hence, they offer an ideal test bench to investigate the applicability of quantum field theories and to predict the properties of the condensates starting from the first principles.

Since the first experimental realizations of dilute Bose-Einstein condensates, a great interest has been focused on this field, resulting in numerous experimental studies concerning, for example, nonlinear dynamics and the elementary excitations of these many-particle quantum systems. The existence of topological phase singularities, quantized vortices, first predicted theoretically and finally observed experimentally in 1999, led to another series of pioneering theoretical and experimental studies.

Several methods to create single-quantum vortices were realized already in 2001 but, however, the puzzle of creating multiply quantized vortices still remained. In this thesis, the so-called topological method to create two and four times quantized vortices is studied in detail. Since the instrumentation required for the experimental realization of the topological method had already been installed in many laboratories, the theoretical predictions of this thesis were experimentally verified shortly after their publication. Multiply quantized vortices are energetically unstable and tend to split into singly quantized vortices. However, the dissipation of energy in the condensates is minimal at low temperatures and, consequently, can lead to long lifetimes for the multiquantum vortices. Nevertheless, one prediction of this thesis is that the lifetimes of doubly quantized vortices are relatively short, owing to the known dynamical instability of the state. The splitting of the doubly quantized vortex has recently been observed experimentally.

The stability of vortices in dilute Bose-Einstein condensates is intimately related to the excitation spectrum of the stationary vortex state. However, developing an accurate, computationally feasible finite-temperature quantum field theory remains an open problem. In this thesis, we study the elementary excitations of an irrotational condensate within a recently developed systematic second order perturbation theory. The collapse and revival of certain elementary excitations is discovered.

The most recent studies of this thesis are devoted to stationary, but rotationally asymmetric vortex states. In weakly interacting condensates, a novel stationary state, a vortex tripole holding finite angular momentum is presented. Also the lowest elementary excitations of the so-called vortex dipole, tripole, and quadrupole states are studied.

Keywords Bose-Einstein condensation, vortex, non-linear phenomena

UDC 530.145:532.527:538.941 | Number of pages 49

ISBN (printed) 951-22-7439-6 | ISBN (pdf) 951-22-7440-X

ISBN (others) | ISSN 1456-3320

Publisher Helsinki University of Technology, Materials Physics Laboratory

Print distribution

☑ The dissertation can be read at http://lib.hut.fi/Diss/

In memoriam
Martti M. Salomaa

Acknowledgements

This work has been carried out in the Materials Physics Laboratory at the Helsinki University of Technology during the years 2002–2004. CSC-Scientific Computing Ltd is acknowledged for computational resources. Financial support from the Finnish Cultural Foundation, the Foundation of Technology, the Research Foundation of Helsinki University of Technology and the Academy of Finland is appreciated.

I thank my supervisor Prof. Martti Salomaa for providing excellent working conditions for the research and Dr. Tech. Sami Virtanen not only for instructing my doctoral thesis, but also for instructing two special assignments and my Master's thesis on Bose-Einstein condensation. I am also indebted to Prof. Mikio Nakahara who offered me an opportunity to collaborate with him in the area of topological vortex creation while I was an undergraduate student. Special expression of gratitude is devoted to Dr. Tomoya Isoshima for his altruistic participation in my research and to Dr. Tapio Simula for constructive discussions. Furthermore, I acknowledge my co-authors Prof. Tetsuo Ohmi, Prof. Kazushige Machida, Dr. Takeshi Mizushima, M.Sc. Hisanori Shimada, Dr. Shin-ichiro Ogawa, and M.Sc. Noaki Matsumoto for their contribution to my research on Bose-Einstein condensation and M.Sc. Juha Vartiainen, M.Sc. Ville Bergholm, and M.Sc. Laura Koponen for collaboration on quantum computation. Also M.Sc. Antti Niskanen, M.Sc. Teemu Ojanen, M.Sc. Niko Marola, and all other people who have joined the inspiring discussions in the Theory Room are acknowledged.

Finally, I warmly thank my family Timo Möttönen, Anita Mikkonen, Milla Möttönen and Katariina Mikkonen for continuous support and my bride-to-be Hanna Kukkonen for her endless love and kindness.

"The meaning of life is
encapsulated in three words:
It's my life."

Otaniemi, November 2004

Mikko Möttönen

List of Publications

This Thesis is a review of the author's work in the field of quantized vortices and elementary excitations in Bose-Einstein condensates of dilute atomic gases. It consists of an overview and the following publications in this field:

I. S-i. Ogawa, M. Möttönen, M. Nakahara, T. Ohmi, and H. Shimada, *Method to create a vortex in a Bose-Einstein condensate*, Phys. Rev. A **66**, 013617 (2002). © 2002 American Physical Society.

II. Mikko Möttönen, Naoki Matsumoto, Mikio Nakahara, and Tetsuo Ohmi, *Continuous Creation of a Vortex in a Bose-Einstein Condensate with Hyperfine Spin F=2*, J. Phys.: Condens. Matter **14**, 13481 (2002). © 2002 IOP Publishing Ltd.

III. M. Möttönen, T. Mizushima, T. Isoshima, M. M. Salomaa, and K. Machida, *Splitting of a doubly quantized vortex through intertwining in Bose-Einstein condensates*, Phys. Rev. A **68**, 023611 (2003). © 2003 American Physical Society.

IV. M. Möttönen, S. M. M. Virtanen, T. Isoshima, and M. M. Salomaa, *Stationary vortex clusters in nonrotating Bose-Einstein condensates*, (2004, submitted to Phys. Rev. A).

V. M. Möttönen, S. M. M. Virtanen, and M. M. Salomaa, *Collapse and revival of excitations in Bose-Einstein condensates*, (2004, accepted to Phys. Rev. A). © 2004 American Physical Society.

Throughout the overview, these papers are referred to by their Roman numerals.

Author's Contribution

The research presented in this dissertation has been carried out in the Materials Physics Laboratory at the Helsinki University of Technology during the years 2002–2004.

The author has been active in writing all the papers I–V and paper V was mainly written by him. In papers I–II, the author has carried out all the numerical computations for which he had developed all the codes and methods. In paper III, the author developed a parallel processing code to solve the equations of motion in three-dimensional complex space and used it to obtain the results. For the paper IV, written based on the author's initial ideas, he developed the method to find the exceptional stationary states of the nonlinear Gross-Pitaevskii equation. In the studies of paper V, the author developed numerical tools to implement the second order perturbation theory for dilute condensates and produced all the results in the paper.

List of Abbreviations

The following acronyms are used in the overview:

BEC	Bose-Einstein condensate
BCS	Bardeen-Cooper-Schrieffer
WFSS	Weak-field seeking state
SFSS	Strong-field seeking state
NS	Neutral state
GP	Gross-Pitaevskii
HFB	Hartree-Fock-Bogoliubov

Contents

1 Introduction

In 1924, Albert Einstein received a request to translate an original work of Satyendra Nath Bose to be published in Zeitschrift für Physik. In the manuscript, Bose gave an alternative derivation of the Planck distribution for the black-body radiation spectrum [1]. Extending Bose's ideas to massive noninteracting particles, Einstein realized that these bosons, particles with integer spin, could condense into the ground state of the system at low temperatures [2, 3]. Referring to the discoverers of the phenomenon, the macroscopic occupation of a single quantum state at low temperatures is called Bose-Einstein condensation.

The original work of Bose and Einstein involved only noninteracting bosons and, hence, it was argued that the condensation may be an anomality of the ideal gas approximation. Nevertheless, Fritz London suggested in 1938 that the then recently found superfluid ^{4}He could be a realization of a Bose-Einstein condensate (BEC) [4, 5]. Since superfluid ^{4}He is a strongly interacting system, it cannot be exhaustively treated with known microscopic theories and the exact characteristics of the lambda transition, *i.e.*, the phase transition into the superfluid state, remain unclear. However, the condensate fraction of superfluid ^{4}He was determined in 1995 using neutron-scattering measurements [6] and Monte Carlo simulations [7]. Due to strong interactions between the ^{4}He atoms, only about 10% of the atoms are in the condensed state and hence superfluid ^{4}He is far from a pure BEC. In addition, the Bardeen-Cooper-Schrieffer (BCS) transition responsible for superconductivity [8] in ordinary superconductors and the phase transitions of superfluid ^{3}He may be interpreted as the formation and simultaneous Bose-Einstein condensation of fermion pairs, but these systems deviate even more from an ideal bosonic gas.

Wide interest was devoted to dilute atomic gases in the 1960's in order to find a quantum system close to the ideal BEC. Before it was possible to reach this goal, major development was to be achieved in the field of trapping and cooling neutral atoms [9–12]. In laser cooling, laser fields with frequency just below the resonance are directed to the atom cloud from all directions in order to slow down the atoms. Whereas the moving particles absorb the Doppler up-shifted photons moving towards them with a higher probability than the Doppler down-shifted photons moving in the same direction with the atoms, the emission of the photons has no preferred direction. It only takes some microseconds to cool the atoms to the "Doppler limit" which is approximately 1 mK at the typical resonance frequencies [13].

For typical peak particle densities $10^{11} - 10^{16}$ cm^{-3}, the condensation temperature T_{BEC} is in the temperature range $10^{-9} - 10^{-4}$ K. Thus, further cooling of the atom cloud is necessary. In principle, the simplest cooling technique is evaporative cooling, in which the atom trap is opened in such a way that the most energetic particles escape from the system which is subsequently thermalized to a lower temperature. Using evaporative cooling, trapped atoms have been cooled down to 50 nK. Other widely used cooling

methods include sub-Doppler laser cooling and laser "sideband" cooling.

The trapping of neutral atoms is conventionally based on shifting of atomic energy levels in magnetic fields produced using coils, laser fields, or both [10–15]. The Zeeman energy of some atomic states increases with increasing field, and vice versa for some other states. The states of the first type are called weak-field seeking states (WFSSs) and the latter ones strong-field seeking states (SFSSs). In addition, there may be states in which atomic spins are orthogonal to the local magnetic field and, hence, these states are unaffected by the magnetic field to the first approximation. These states are called neutral states (NSs). The Zeeman energy, responsible for the confinement of the atoms, is mainly determined by the orientation of the electronic spins since the nuclear magnetic moment is negligibly small compared with the magnetic moment of the valence electron. However, the nuclear spin has a strong effect on the orientation of the electron spin for the alkali atoms in weak magnetic traps. For example, the ^{23}Na and ^{87}Rb atoms may have hyperfine spin* 1, for which there exists one WFSS, one SFSS and one NS.

A rather new result [16] of classical electromagnetic theory forbids the magnetic field to have a maximum in free space. Thus, only WFSSs can be trapped in a purely magnetic trap. On the other hand, all the hyperfine states can be trapped in optical traps which are realised with lasers having a frequency far below (red detuned) or above (blue detuned) the resonance frequency, giving rise to a conservative attractive or a repulsive force, respectively [14,15]. Since the optical potential is proportional to the laser intensity, the laser field should be inhomogeneous in space. Combinations of magnetic and optical traps are so-called magneto-optical traps [17], for which the frequency of the spatially homogeneous laser field is close to resonance and, in addition, there is a weak inhomogeneous magnetic field which adjusts the resonance frequency of the atoms, resulting in the strength of the optical potential to be inhomogeneous. However, the energy transfer and spin flips due to nearly resonant laser field render it impossible to achieve condensation in magneto-optical traps.

In the beginning of the 90's, the most promising candidates for neutral atoms to form a gaseous BEC were the alkali atoms, since their atomic excitation spectra dovetailed with the frequencies of the available lasers. Finally in 1995, a breakthrough took place when Andersson *et al.* at JILA†, Davis *et al.* at MIT‡ and Bradley *et al.* at Rice University managed to observe BECs of ^{87}Rb [18], ^{23}Na [19] and ^{7}Li [20] atoms in magnetic traps, respectively. These trail-blazing experiments gave a remarkable boost to both the experimental and theoretical investigation of BECs in alkali atom vapours. To date, over 100 different groups have achieved atomic condensation and new atomic species have been added to the family of BECs including spin-polarized hydrogen [21], ^{85}Rb [22],metastable ^{4}He [23, 24], ^{41}K [25] and ^{133}Cs [26].

In December 2003, the observation of Bose-Einstein condensation of both $^{40}K_2$ and

*Hyperfine spin 2 is also possible for these atoms.

†Joint Institute for Laboratory Astrophysics, University of Colorado at Boulder.

‡Massachusetts Institute of Technology.

$^6Li_2$ molecules was reported [27–29] and already in January 2004 the observation of condensed fermionic atom pairs of ^{40}K [30], "the Fermi condensate", attracted worldwide media publicity and scientific attention. The difficulties in imaging the fermionic condensate were overcame in the BCS-BEC crossover by changing the interaction between the atoms in a such way that molecular BEC was formed and the BEC was then observed. It was also shown that without the fermionic condensate the formation of molecules is much slower and actually the observed BEC corresponds to the original fermionic condensate. The reason why this discovery is especially inspiring, is that the temperature at which the condensation takes place is as high as 7% of the Fermi temperature. In comparison with the Fermi temperatures of present superconductors, the 7% would correspond to a temperature much higher than room temperature.

The Bose-Einstein condensate of dilute alkali atom gases is not only interesting since it better fits the original work of Bose and Einstein than superfluid ^{4}He, superconductors or superfluid ^{3}He, but also since it is directly observable using optical imaging techniques and it forms a highly controllable macroscopic quantum system. The magnetic and optical trapping potentials may be adjusted to have a multitude of shapes and the interactions between the atoms may be tuned in a wide range using Feshbach resonances [31,32]. Even the sign of the s-wave scattering length describing the interactions between the atoms in these dilute BECs at ultralow temperatures [33, 34] can be reversed. These peculiar properties of dilute BECs render them ideal systems on which to develop and test thermal quantum field theories [35].

In the zero-temperature limit, it is commonly assumed that all the atoms are in the condensed state of the WFSS and the system may be characterized by a single complex field called the order parameter. The squared magnitude of the order parameter yields the particle density and its phase gradient is proportional to the coherent particle flow of the condensate. The dynamics of the order parameter are governed by the Gross-Pitaevskii (GP) equation whereas the excitations of the stationary states are described by the Bogoliubov eigenvalue equations which have been proven to be highly accurate for temperatures $T \ll T_{\rm BEC}$ [36–39]. Due to interactions between the particles, the GP equation is nonlinear and, therefore, analytically solvable only in rare cases. Since the Bogoliubov equations contain the stationary-state order parameter, they can only be solved analytically in just the same cases as also the GP equation. Hence, numerical tools are needed, in general, to study the characteristics of BECs even at zero temperature.

The simplest way to take the finite temperature into account is to calculate the number of thermal atoms using the excitations obtained from the Bogoliubov equations in the Bose distribution function and adjusting the number of condensed particles such that the total number of particles matches the desired value. A more accurate theory is obtained within the so-called Popov approximation to the Hartree-Fock-Bogoliubov (HFB) theory [40, 41]. In the HFB-Popov theory, both the GP equation and the Bogoliubov equations are generalized to include an effective potential arising from the distribution of the thermal particles. These equations are solved self-consistently for a

given total number of particles. In comparison with the measured excitation energies at JILA [42], the HFB-Popov theory yields the same energies within an accuracy of 5% for temperatures $T < 0.6T_{\rm BEC}$ [43].

A lot of theoretical effort has been devoted to explaining the anomalous behaviour of the excitation energies above $0.6T_{\rm BEC}$ using static [44–51] and kinetic [52–56] theories. The second order theory presented in Refs. [50, 51] uses systematic perturbation theory to take into account the interaction terms in the Hamiltonian. Recently, this theory was extended to include time-dependent external perturbations used to drive the system in the experiments [42], leading to fair agreement with the measured energies and the damping rates for the collective modes [57, 58]. The perturbation is only introduced to excite the measured density oscillations of the condensate and is, of course, absent in thermodynamic equilibrium. Without the time-dependent perturbation, the second order theory, however, does not show the anomalous energy shift. Thus the energy shift may be argumented to be a result of the measurement techniques rather than characteristics of the excitations in the thermal equilibrium. In the light of these results, it is possible that the HFB-Popov theory describes the elementary excitations in the thermodynamic equilibrium quite accurately even at temperatures above $0.6T_{\rm BEC}$.

The implementation of the second order theory is computationally challenging and there exist only a few numerical investigations thereof in the literature [57, 59, 60]. In Paper V, the second order theory is applied for the first time to pancake-shaped condensates and the excitation spectra and the dynamics of the excitations are investigated. The dynamics of certain modes are demonstrated to show a collapse and revival phenomenon which has been mentioned in the previous literature [50, 51], but not calculated exactly. Moreover, the second order theory is used to qualitatively explain the recent observation of the Beliaev process in the dynamics of the so-called scissors mode [61, 62].

One fundamental question is whether the atomic BECs are superfluid. Superfluid properties are closely associated with the ability to sustain frictionless flow, which is related to the stability of vortices. Quantized vortices are topological defects in the complex-valued order parameter. There is an integer multiple, the quantum number of the vortex, of 2π phase winding encircling a vortex which induces an azimuthal particle flow, i.e., angular momentum. Since the phase winding is discrete and the order parameter is a continuous function, the phase winding is the same along every loop encircling close enough to the vortex line. This implies a phase singularity along the vortex axis, where the continuous order parameter must vanish.

Quantized vortices were first discovered in superconductors [63] (1964) using neutron diffraction and in superfluid ^{4}He [64] (1974) with a photographic technique making use of electron bubbles trapped in vortex cores. After the first physical realizations of alkali atom BECs, there was a wide debate that vortices should also occur as excitations of the coherent condensate. Many methods were suggested to create vortices and in 1999 the first vortex was created in an alkali atom BEC [65] using a phase imprinting method. In the phase imprinting method, the order parameter obtains its phase from that of

an additional laser field. Vortices may also be created by stirring the condensate with a focused laser beam [66–68] or by rotating the magnetic trapping potential [69]. However, vortices thus created were all single-quantum vortices. Since the quantum number of the vortex is proportional to the angular momentum it sustains, a naive guess would be that by increasing the rotation frequency of the trapped condensate, one could create multiquantum vortices. This turned out not to be the case, but instead, vortex lattices of up to about 100 singly quantized vortices were observed [70] due to the fact that the energy of a vortex is roughly proportional to its squared quantum number.

In Refs. [71,72], a topological method to create multiquantum vortices was proposed. In this method, the BEC is confined in a magnetic trap and it was shown that a multiquantum vortex can be created by reversing the bias magnetic field of the Ioffe-Pritchard trap [14,15]. In addition to the magnetic trap, a narrow optical potential was introduced and focused into the center of the condensate to avoid the spin flips which may take place when the magnetic field vanishes. The laser field was in the core of the multiquantum vortex created and hence, strictly speaking, a persistent current analogous to the ones in superconducting rings was created rather than a vortex. This method has not been verified experimentally since the requirement of the narrow laser beam causes additional difficulties. Nevertheless, it is shown in Papers I and II that roughly half of the particles escape from the trap in the absence of the laser provided that the bias field is reversed with the right speed. Using the scenario of Papers I and II, the first vortices with quantum numbers two and four were experimentally observed in dilute BECs [73].

The experimentally realized double-quantum vortices were observed to have a lifetime of at least about 20 ms. Since the doubly quantized vortex state of the harmonically trapped BEC is known to be dynamically unstable [74], *i.e.*, small perturbations can grow exponentially in time, the vortex was expected to split into two singly quantized vortices. In Paper III, this splitting is investigated in cigar-shaped condensates used in the actual experiments and it was observed that the two vortex lines intertwine as they split. This intertwining is a purely three-dimensional phenomenon which remains to be verified in the experiments. However, the actual splitting has recently been observed in cigar-shaped BECs [75] in harmony with the results of Paper III.

In Paper IV, some rotationally asymmetric stationary states of pancake-shaped BECs are investigated. The existence and dynamical stability of two of these states, namely a vortex dipole and quadrupole, was first reported in Refs. [76, 77]. Nevertheless, the energetic stability of these states remained unanswered. In our studies, the states proved to be both energetically and dynamically unstable. Moreover, a novel state, vortex tripole, involving one vortex in the center of the BEC and two off-axis antivortices at the same distance from the center was introduced. All the three vortices in the tripole are collinear. If the distance between the vortex and the antivortices is small (large), the antivortices precess in the clockwise (counterclockwise) direction. Hence, there must exist a certain distance over which the state is stationary. Moreover, the stationary vortex clusters turned out not to be local minima of the free energy, but rather saddle points.

Hence, the most promising circumstances to experimentally generate these structures are in weakly dissipative condensate systems, using phase-imprinting techniques.

The structure of this overview is the following. In Sec. 2, we discuss the zero-temperature mean-field theory for weakly interacting BECs. We introduce the scalar order parameter and review the derivation of the GP and the Bogoliubov equations. We also present these equations for a spinor-valued order parameter and discuss the topological method to create multiply quantized vortices. Furthermore, the splitting of doubly quantized vortices and the asymmetric stationary states are investigated.

Section 3 is devoted to the presentation of the second order theory for Bose-Einstein condensed vapours. By using systematic perturbation theory we derive the GP and Bogoliubov equations more rigorously than in Sec. 2. They are the starting point for the second order theory, *i.e.*, the zeroth order approximation. The first order theory turns out to be essentially the HFB-theory for which, motivated by the complete second order theory, the Popov approximation can be applied. Finally, the energies and decay of elementary excitations is studied within the second order theory.

2 Zero-Temperature Mean-Field Theory

In this section, we derive the GP equation to solve the dynamics of the BECs and the Bogoliubov equations to find the excitation spectra of stationary states. The derivation is accomplished using the field operator and assuming that it is fully described by the condensate order parameter at zero temperature. A more rigorous derivation of the equations is given in Sec. 3. The GP and Bogoliubov equations are used in Secs. 2.2 and 2.4 to study the properties of stationary vortex clusters and doubly quantized vortices, respectively. In Sec. 2.3, we present the GP equation for a spinor condensate with the hyperfine spin $F = 2$ and show how it can be used to create a fourfold quantized vortex state.

2.1 Scalar condensates

In this subsection, we consider a BEC trapped in a magnetic potential for which the magnetic field does not vanish in the region of the BEC. Hence, only the WFSS is trapped and spin flips to the other spin states may be taken to be negligible. The WFSS can be described by a single complex-valued order parameter $\Phi(\mathbf{r})$, which is the quantum expectation value of the field operator

$$\hat{\Psi}(\mathbf{r}) = \sum_{i=0}^{\infty} \psi_i(\mathbf{r}) a_i, \tag{2.1}$$

where the single-particle wave functions $\{\psi_i(\mathbf{r})\}$ form an L^2-complete orthonormal basis and the symbol a_i denotes the usual bosonic annihilation operators of the ith single-particle state. Due to the spontaneously broken gauge symmetry [78,79], the expectation value of the field operator is nonzero in the presence of the condensate. The absolute value of the order parameter yields the density of the condensed particles $n_c = |\Phi(\mathbf{r})|^2$ and, hence, the order parameter may be presented as

$$\Phi(\mathbf{r}) = \sqrt{n_c(\mathbf{r})} e^{iS(\mathbf{r})}, \tag{2.2}$$

where we have introduced the phase function $S(\mathbf{r})$. The velocity of the superfluid flow is defined as

$$\mathbf{v} = \frac{\hbar \nabla S(\mathbf{r})}{m}. \tag{2.3}$$

These equations also hold at finite temperatures, but in that case the total number of particles N also includes contributions from the thermal gas.

In terms of the field operator in Eq. (2.1), the Hamiltonian of the many-particle system is given by

$$\hat{H} = \int \hat{\Psi}^\dagger(\mathbf{r}) \hat{h}(\mathbf{r}) \hat{\Psi}(\mathbf{r}) d\mathbf{r} + \frac{1}{2} \iint \hat{\Psi}^\dagger(\mathbf{r}) \hat{\Psi}^\dagger(\mathbf{r}') V(\mathbf{r} - \mathbf{r}') \hat{\Psi}(\mathbf{r}') \hat{\Psi}(\mathbf{r}) d\mathbf{r} d\mathbf{r}', \tag{2.4}$$

where the operator $\hat{h}(\mathbf{r})$ is the single-particle Hamiltonian in the Schrödinger picture and $V(\mathbf{r}-\mathbf{r}')$ is the interatomic two-body interaction potential. In dilute BECs, the interaction potential may be approximated by an effective delta-function potential [14,15]

$$V(\mathbf{r}-\mathbf{r}') = g\delta(\mathbf{r}-\mathbf{r}'), \tag{2.5}$$

where the interaction strength g may be expressed using the two-body s-wave scattering length a and the atomic mass m as

$$g = \frac{4\pi\hbar^2 a}{m}. \tag{2.6}$$

This approximation does not hold at high energies, which leads to divergences of certain quantities which, however, can be renormalized properly. The single-particle Hamiltonian may be written as

$$\hat{h}(\mathbf{r}) = -\frac{\hbar^2\nabla^2}{2m} + V_{\text{trap}}(\mathbf{r}), \tag{2.7}$$

where the trapping potential $V_{\text{trap}}(\mathbf{r})$ consists of a magnetic field and, possibly, an additional optical field. However, the optical field should be non-confining or it should be applied after the condensate has relaxed into a pure WFSS for the scalar condensate approximation to be valid.

We use the Heisenberg picture where time development is contained in the operators. In the Heisenberg picture, the temporal development of operators is obtained from the Heisenberg equation of motion

$$i\hbar\partial_t\hat{\Psi}(\mathbf{r},t) = [\hat{\Psi}(\mathbf{r},t), \hat{H}]. \tag{2.8}$$

The canonical commutation relations of the annihilation and the creation operators

$$[a_i, a_j^\dagger] = \delta_{ij}, \quad [a_i^\dagger, a_j^\dagger] = 0, \quad \text{and} \quad [a_i, a_j] = 0 \tag{2.9}$$

yield the equal-time commutation relations for the field operators

$$[\hat{\Psi}(\mathbf{r}), \hat{\Psi}^\dagger(\mathbf{r}')] = \delta(\mathbf{r}-\mathbf{r}'), \quad [\hat{\Psi}(\mathbf{r}), \hat{\Psi}(\mathbf{r}')] = 0, \quad \text{and} \quad [\hat{\Psi}^\dagger(\mathbf{r}), \hat{\Psi}^\dagger(\mathbf{r}')] = 0. \tag{2.10}$$

Using the commutation relations (2.10) and the interatomic potential of Eq. (2.5), the Heisenberg equation of motion for the field operator assumes the form

$$i\hbar\partial_t\hat{\Psi}(\mathbf{r},t) = \left[\hat{h}(\mathbf{r},t) + g\hat{\Psi}^\dagger(\mathbf{r},t)\hat{\Psi}(\mathbf{r},t)\right]\hat{\Psi}(\mathbf{r},t). \tag{2.11}$$

In the zero-temperature limit, thermal and quantum fluctuations of the field operator are negligible and the field may be accurately described by its expectation value, *i.e.*, the equation of motion for the order parameter $\Phi(\mathbf{r},t) = \langle\hat{\Psi}(\mathbf{r},t)\rangle$ is obtained from Eq. (2.11) by replacing the field operator with the order parameter. This substitution yields the GP equation

$$i\hbar\partial_t\Phi(\mathbf{r},t) = \left[-\frac{\hbar^2\nabla^2}{2m} + V_{\text{trap}}(\mathbf{r}) + g|\Phi(\mathbf{r},t)|^2\right]\Phi(\mathbf{r},t), \tag{2.12}$$

which was originally independently obtained by Gross [80] and Pitaevskii [81]. Owing to the non-linear term arising from the interactions between the atoms, the GP equation is also referred to as a nonlinear Schrödinger equation. This terminology may be somewhat misleading, since the Schrödinger equation for any pure quantum state is always linear. However, one must recall that the GP equation is not an equation for a pure quantum state of the system, but rather an effective equation for the matter field describing the average particle distribution and velocity of the BEC.

In addition to the temporal evolution of the BEC, the GP equation may be used to find certain stationary states of the form $\Phi(\mathbf{r},t) = e^{-i\mu t/\hbar}\Phi(\mathbf{r})$ of the system, for which the chemical potential is denoted by μ. In particular, the ground state of the system of N particles is obtained by finding the stationary state corresponding to the minimum of the energy functional

$$E(\Phi) = \int \Phi^*(\mathbf{r}) \left[-\frac{\hbar^2\nabla^2}{2m} + V_{\text{trap}}(\mathbf{r}) + \frac{g}{2}|\Phi(\mathbf{r})|^2 \right] \Phi(\mathbf{r}) d\mathbf{r}, \tag{2.13}$$

which may be obtained from Eq. (2.4) by replacing the field operator by the order parameter. Since the absolute squared value of the order parameter yields the particle density, the minimization must be accomplished under the constraint $\int |\Phi(\mathbf{r})|^2 d\mathbf{r} = N$.

The elementary excitations of the stationary states play an important role in the study of BECs [14,15]. These excitations are defined as small fluctuations whose energies and shapes may be used to analyze the behaviour of the BECs exposed to small external perturbations [74]. Let us write the field operator in terms of the order parameter and the fluctuation operator as $\hat{\Psi}(\mathbf{r},t) = \Phi(\mathbf{r},t) + \hat{\psi}(\mathbf{r},t)$. By neglecting all but linear terms of $\hat{\psi}(\mathbf{r},t)$ in the Heisenberg equation of motion we obtain

$$i\hbar\partial_t\hat{\psi}(\mathbf{r},t) = \left[-\frac{\hbar^2\nabla^2}{2m} + V_{\text{trap}}(\mathbf{r}) + 2g|\Phi(\mathbf{r})|^2 \right] \hat{\psi}(\mathbf{r},t) + g\Phi^2(\mathbf{r})\hat{\psi}^\dagger(\mathbf{r},t). \tag{2.14}$$

By inserting the Bogoliubov transformation

$$\hat{\psi}(\mathbf{r},t) = \sum_k [u_k(\mathbf{r})e^{-i(\varepsilon_k+\mu)t/\hbar}a_k + v_k^*(\mathbf{r})e^{i(\varepsilon_k-\mu)t/\hbar}a_k^\dagger], \tag{2.15}$$

to this equation, we obtain the Bogoliubov equations

$$\begin{pmatrix} \mathcal{L}(\mathbf{r}) & \mathcal{M}(\mathbf{r}) \\ -\mathcal{M}^*(\mathbf{r}) & -\mathcal{L}(\mathbf{r}) \end{pmatrix} \begin{pmatrix} u_k(\mathbf{r}) \\ v_k(\mathbf{r}) \end{pmatrix} = \varepsilon_k \begin{pmatrix} u_k(\mathbf{r}) \\ v_k(\mathbf{r}) \end{pmatrix}, \tag{2.16}$$

where $u_k(\mathbf{r})$ and $v_k(\mathbf{r})$ are the quasiparticle amplitudes, ε_k the quasiparticle energies with respect to the chemical potential μ, and where the operators $\mathcal{L}(\mathbf{r}) = \hat{H}^{\text{sp}} - \mu + 2g|\Phi(\mathbf{r})|^2$ and $\mathcal{M}(\mathbf{r}) = g\Phi^2(\mathbf{r})$ have been introduced. In addition, the quasiparticle amplitudes must satisfy the orthogonality relations

$$\int \left[u_k^*(\mathbf{r})u_j(\mathbf{r}) - v_k^*(\mathbf{r})v_j(\mathbf{r}) \right] d\mathbf{r} = \delta_{jk} \tag{2.17}$$

for the Bogoliubov transformation to be canonical.

The stationary states of any system correspond to a local minimum, a local maximum or a saddle point of the energy functional. Once the stationary solution of the GP equation is found, the Bogoliubov equations may be used to analyse the energetic stability of the state; if all the modes have a positive energy, the state must be a local minimum of energy. On the other hand, the states having negative-energy excitations are always saddle points of the energy functional. It should be noted that the Bogoliubov equations are not Hermitian and, therefore, the existence of imaginary energy eigenvalues is not excluded. For example, the doubly quantized vortex state, $\Phi(\mathbf{r}) = \sqrt{n_{\rm c}(r,z)}e^{i4\pi\theta}$ expressed using the cylindrical coordinates (r,θ,z), is known to sustain imaginary-frequency modes [74] which imply the dynamical instability of the state, *i.e.*, infinitesimal perturbations can lead to exponentially growing fluctuations. In the case of a doubly quantized vortex, these fluctuations tend to split the vortex into two single-quantum vortices.

2.2 Vortex states

In this subsection, we focus on stationary states of pancake-shaped BECs that contain several vortices*. The external potential used to trap the condensate may be accurately approximated with a harmonic potential

$$V_{\rm trap}(\mathbf{r}) = \frac{m\omega_x^2}{2}x^2 + \frac{m\omega_y^2}{2}y^2 + \frac{m\omega_z^2}{2}z^2, \tag{2.18}$$

where ω_i is the oscillator frequency in the direction i. The geometry of the pancake-shaped system is chosen such that $\omega_z \gg \omega_x \sim \omega_y$ and, hence, the z dependence of the order parameter may be taken to be independent of the other coordinates [74]. To be more precise, we approximate $\Phi(\mathbf{r}) = \Phi(r,\theta)\sigma(z)$ expressed using the cylindrical coordinates (r,θ,z). By multiplying the GP equation with normalized $\sigma^*(z)$ from the left-hand side and integrating over z, it becomes effectively two-dimensional

$$i\hbar\partial_t\Phi(r,\theta,t) = \left[-\frac{\hbar^2\nabla^2}{2m} + V_{\rm trap}(\mathbf{r}) + g_{\rm 2D}|\Phi(r,\theta,t)|^2 + E_z\right]\Phi(r,\theta,t), \tag{2.19}$$

where $g_{\rm 2D} = g\int|\sigma(z)|^4dz/\int|\sigma(z)|^2dz$ and E_z is the single-particle energy in the z direction. Actually, the same equation is obtained, apart from different scaling of the interaction parameter, by assuming a homogeneous condensate along z, *i.e.*, $\omega_z = 0$.

The easiest example of a vortex line in a BEC is the one located at the center of a rotationally symmetric condensate for which $\omega_r := \omega_x = \omega_y$. In this case, the phase function of the order parameter is of the form $S(\mathbf{r}) = \kappa\theta$. Here, the winding number of the vortex is denoted by κ and the absolute value of the order parameter is obtained from the state having the lowest energy and being of the form $\Phi(r,\theta) = |\Phi(r)|e^{i\kappa\theta}$. For $\kappa = 0$, there is no vorticity and the solution found is the global minimum of energy and

*For a review on vortices in dilute BECs, see Ref. [82].

for other winding numbers the state found is a saddle point of the energy [82]. Since the phase of the order parameter is not well defined along the vortex axis where the phase singularity occurs, the continuous order parameter must vanish there. The velocity field for the state $\Phi(r,\theta) = |\Phi(r)|e^{i\kappa\theta}$ can be calculated from Eq. (2.3) as

$$\mathbf{v} = \frac{\hbar\kappa}{mr}\boldsymbol{\theta}, \tag{2.20}$$

where $\boldsymbol{\theta}$ is the unit vector in the azimuthal direction. The velocity of the vortex diverges along the vortex line but, however, the kinetic energy does not diverge since the particle density vanishes. Equation (2.20) shows that the particles flow encircling the vortex line, which is analogous to a classical vortex. The average angular momentum per particle related to the vortex state in question is $\langle\Phi|L_z|\Phi\rangle/N = \hbar\kappa$ along the z direction.

In general, the position of a vortex line is defined as the location of the phase singularity. In practice, the vortices are commonly observed as holes in the particle-density profile, but in numerical simulations of the GP equation, of course, the phase of the order parameter may also be examined directly. In Fig. 2.1(a), the particle density and the phase of a stationary vortex dipole state is illustrated. The radius of the vortex core is approximately given by a parameter called the healing length

$$\xi = (8\pi n_{\rm c} a)^{-1/2}, \tag{2.21}$$

where the density of the condensed particles, is regarded as the average background density at the same position as the vortex line but in the absence of the vortex. Since the condensate density in the ground state is smaller at the edges of the condensate than in the middle, the further away the vortex is located from the center of the condensate, the larger the vortex core is. This phenomenon is shown in Fig. 2.1(b), in which a stationary vortex tripole is presented.

A condensate state containing only a single vortex is stationary only if the vortex is located at the center of the condensate since off-axis vortices tend to precess in the direction of the superfluid flow, *i.e.*, clockwise for an antivortex and counterclockwise for a vortex, see Eq. (2.20). This precession is due to the buoyancy force acting on the vortex which arises from the fact that the energy of the system decreases as the radial distance of the vortex from the center of the trap increases. Nevertheless, the energy of the system must be conserved during temporal evolution and the vortex precesses along a constant-energy curve. The force balancing the buoyancy force is the so-called Magnus force [83–86] which arises from the precessional motion and circulation of the vortex line. To a good approximation, the Magnus force may be written as [14, 15]

$$\mathbf{F}_{\rm Mag} = m n_{\rm c}(\boldsymbol{\kappa} \times \mathbf{v}_{\rm core}), \tag{2.22}$$

where the vorticity vector $\boldsymbol{\kappa} = 2\pi\hbar\kappa\mathbf{z}/m$, and the velocity of the vortex core is denoted by $\mathbf{v}_{\rm core}$. In conclusion, the faster an off-axis vortex precesses, the greater the energy gradient is in the radial direction.

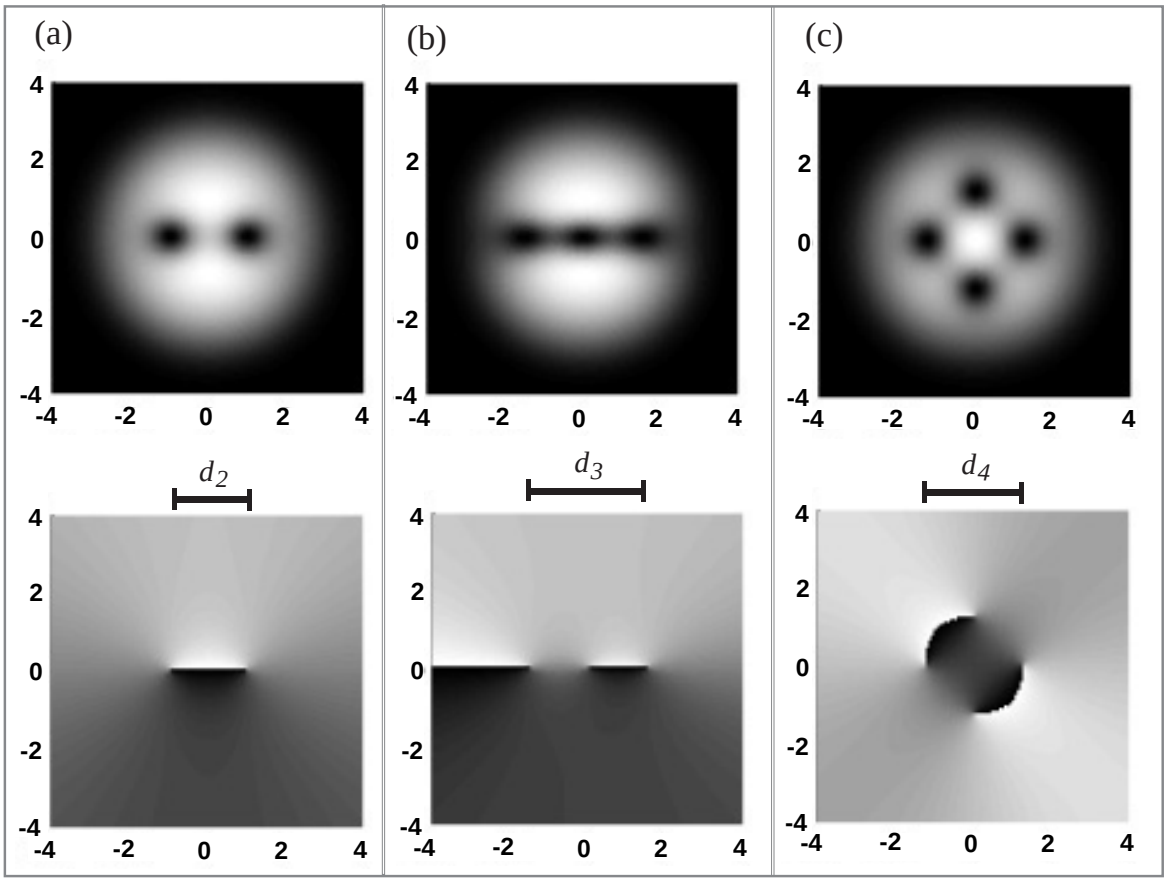

Figure 2.1: Density profiles (upper panels) and phase functions $S(\mathbf{r})$ (lower panels) for a vortex dipole (a), tripole (b) and quadrupole (c). The spatial coordinates are in units of micrometers.

Let us now consider a vortex dipole, such as that in Fig. 2.1(a). The distance between the vortex and the antivortex is denoted by d_2 and the energy $E_2(d_2)$ is defined as the energy minimum with the restriction that the distance of the phase singularities is d_2. The definitions are analogous for the vortex tripole and quadrupole, see Figs. 2.1(b)-(c). The ground state of the system is obtained in the limit $d_2 \to 0$ for the vortex dipole and, hence, the energy gradient with respect to the distance is positive for sufficiently small d_2. On the other hand, the ground state is also obtained in the limit $d_2 \to \infty$. Thus, there must exist at least one point d_2^e which is a local maximum of energy with respect to d_2. In Fig 2.2, we have plotted the energies of a vortex dipole, tripole and quadrupole as functions of the vortex separations. A local maximum is seen in each of the graphs. The maxima indicate the existence of stationary states near these extremal points.

To prove that these stationary states do exist, we used the wave functions obtained from the energy minimization procedure as the initial conditions and used the method of steepest descent to find the stationary states. The method of the steepest descent is

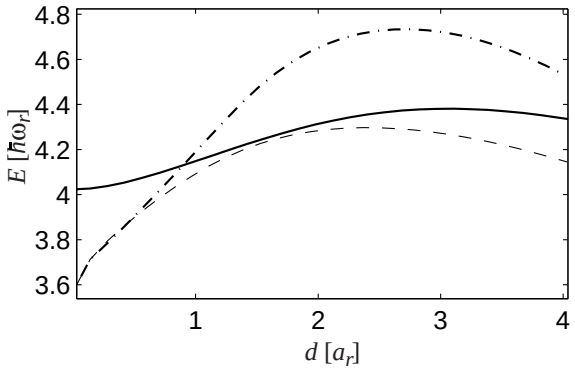

Figure 2.2: Energy of the vortex dipole (dashed line), tripole (solid line) and quadrupole (dash-dotted line) as functions of the distances d_2, d_3 and d_4, respectively.

based on moving towards the negative gradient of the functional $F[\Phi]$ to be minimized. Since the functionals we consider are invariant under conjugation, *i.e.*, $F[\Phi] = F[\Phi^*]$, the variation of the functional with respect to $\Phi(\mathbf{r})$ is obtained by functional differentiation with respect to $\Phi^*(\mathbf{r})$. For example, the left-hand side of the GP equation (2.12) is obtained as

$$\nabla_{\Phi^*} E[\Phi] =: \lim_{\delta\Phi^*\to 0} \frac{E[\Phi, \Phi^* + \delta\Phi^*] - E[\Phi, \Phi^*]}{\delta\Phi^*} = H[\Phi]\Phi, \tag{2.23}$$

where $E[\Phi]$ is the energy functional in Eq. (2.13) and $H[\Phi]$ is the nonlinear Hamiltonian of the the GP equation (2.12). Since the number of particles is to be conserved in the minimization process, we minimized $E[\Phi] - \mu N$ instead of just the energy functional and the gradient becomes $(H[\Phi] - \mu)\Phi(\mathbf{r})$. The Lagrange multiplier μ must be adjusted in such a way that the resulting total number of particles is N, or if the number of the particles is allowed to change during the minimization process, we may fix μ. Since the norm $\mathcal{F}[\Phi] = ||(H[\Phi] - \mu)\Phi||^2$ vanishes for stationary states and is positive for all other states, stationary states may be found by minimizing the norm using functional differentiation

$$\nabla_{\Phi^*} \mathcal{F}[\Phi] = \left\{ (H[\Phi] - \mu)^2 + 2g\mathrm{Re}\left[\Phi^*(H[\Phi] - \mu)\Phi\right] \right\} \Phi. \tag{2.24}$$

Even though the Hamiltonian operator $H[\Phi]$ is nonlinear, it is treated in Eq. (2.24) as a linear operator which only depends on the order parameter Φ, not on the state it operates to. The convergence of the method towards the stationary vortex cluster states is monotonic and errors $\mathcal{F}[\Phi]/(N\mu^2)$ less than 10^{-21} were obtained for all the states in question.

The method of steepest descent for the ground state of the GP equation has been studied in Ref. [87], in which also a Sobolev gradient preconditioning is presented to enhance numerical convergence. Excited stationary states were also studied in the context

of nonlinear optics by directly minimizing the error. However, this direct minimization was not used when the vortex dipole and quadrupole were introduced in Refs. [76,77], in which it was argued that the configurations were dynamically stable in certain parameter ranges. In Paper IV, the energetic instability of these states was shown by calculating the energy graphs of Fig. 2.2 from the GP equation and by solving the Bogoliubov equations which yielded the excitation spectra for the vortex dipole, tripole and quadrupole with negative-energy modes. The spectra of all the three cluster configurations showed also imaginary eigenvalues, suggesting that the stationary states are dynamically unstable; certain infinitesimal perturbations of the stationary state lead to finite perturbations during the temporal evolution. This observation was verified by adding the imaginary frequency modes to the initially stationary vortex clusters, which resulted in peculiar temporal development for each of the configurations. The vortex dipole was observed to precess and, hence, to preserve its shape. On the other hand, the vortices in the quadrupole moved towards the center of the condensate, mutually annihilating each other. Finally, one of the antivortices in the vortex tripole escaped to the edge of the condensate, while the remaining two vortices formed a vortex dipole. Thus the vortex dipole may be considered as the most stable configuration studied in this thesis.

2.3 Spinor condensates

The actual nature of the alkali atom BECs is a spinor field, since the atoms possess spin degrees of freedom, *e.g.*, the nuclear spin of ^{87}Rb and ^{23}Na is $I = 3/2$ which together with the electron spin $J = 1/2$ results in a hyperfine spin $F = 1$ or 2. In this subsection, we discuss the case of a hyperfine spin $F = 2$ since the phenomena observed in this case also include those of $F = 1$. The order parameter is given by

$$\Phi(\mathbf{r}) = \sum_{k=-F}^{F} \Phi_k(\mathbf{r})|k\rangle, \tag{2.25}$$

where we have chosen the spinor basis $\{|k\rangle\}$ such that it is the eigenbasis of the z component of the hyperfine spin operator F_z with eigenvalues $\{k\}$; $F_z|k\rangle = k|k\rangle$. In this basis, we may also write the order parameter as a vector $\Phi = (\Phi_2, \Phi_1, \Phi_0, \Phi_{-1}, \Phi_{-2})^T$ and the spin operators as

$$F_x = \begin{pmatrix} 0 & 1 & 0 & 0 & 0 \\ 1 & 0 & \upsilon & 0 & 0 \\ 0 & \upsilon & 0 & \upsilon & 0 \\ 0 & 0 & \upsilon & 0 & 1 \\ 0 & 0 & 0 & 1 & 0 \end{pmatrix}, F_y = i \begin{pmatrix} 0 & -1 & 0 & 0 & 0 \\ 1 & 0 & -\upsilon & 0 & 0 \\ 0 & \upsilon & 0 & -\upsilon & 0 \\ 0 & 0 & \upsilon & 0 & -1 \\ 0 & 0 & 0 & 1 & 0 \end{pmatrix}, F_z = \begin{pmatrix} 2 & 0 & 0 & 0 & 0 \\ 0 & 1 & 0 & 0 & 0 \\ 0 & 0 & 0 & 0 & 0 \\ 0 & 0 & 0 & -1 & 0 \\ 0 & 0 & 0 & 0 & -2 \end{pmatrix},$$

where $\upsilon = \sqrt{3/2}$.

The Gross-Pitaevskii equation for the spinor condensates is of the form [88,89]

$$\begin{aligned} i\hbar\frac{\partial}{\partial t}\Phi_m = & \left[-\frac{\hbar^2}{2m}\nabla^2 + V_{\rm opt}(r) + g_1\sum_{n=-2}^{2}|\Phi_n|^2\right]\Phi_m \\ & + \sum_{k\in\{x,y,z\}}\sum_{n,p,q=-2}^{2} g_2\left[\Phi_n^\dagger(F_k)_{np}\Phi_p\right](F_k)_{mq}\Phi_q \\ & + \sum_{n,p,q=-2}^{2} 5g_3\Phi_n^\dagger\langle\, 2m2n|00\,\rangle\langle\, 00|2p2q\,\rangle\Phi_p\Phi_q \\ & + \sum_{k\in\{x,y,z\}}\sum_{n=-2}^{2}\frac{1}{2}\hbar\omega_{{\rm L}k}(F_k)_{mn}\Phi_n, \end{aligned} \tag{2.27}$$

where the optical potential $V_{\rm opt}(\mathbf{r})$ is independent of the spin degree of freedom and the Larmor frequencies $\omega_{{\rm L}k} = \mu_{\rm B}B_k/\hbar$ are described by the Bohr magneton $\mu_{\rm B}$ and the external magnetic field $\mathbf{B}$. The projection of the two-atom state $|2p2q\rangle$ to the two-atom state with vanishing total spin is denoted by $\langle\, 00|2p2q\,\rangle$. The three interaction parameters

$$g_1 = \frac{4\pi\hbar^2}{m}\frac{4a_2+3a_4}{7},\; g_2 = -\frac{4\pi\hbar^2}{m}\frac{a_2-a_4}{7},\; g_3 = \frac{4\pi\hbar^2}{m}\left(\frac{a_0-a_4}{5} - \frac{2a_2-2a_4}{7}\right),$$

are obtained using the s-wave scattering lengths $a_0 = 4.73$ nm, $a_2 = 5.00$ nm and $a_4 = 5.61$ nm for the different channels of ^{87}Rb [88]. The last term in Eq. (2.27), containing the contribution from the magnetic trap, may be expressed as the matrix

$$\mathcal{B} = \frac{\mu_{\rm B}}{2}\begin{pmatrix} 2B_z & B_\perp e^{i\phi} & 0 & 0 & 0 \\ B_\perp e^{-i\phi} & B_z & \sqrt{\frac{3}{2}}B_\perp e^{i\phi} & 0 & 0 \\ 0 & \sqrt{\frac{3}{2}}B_\perp e^{-i\phi} & 0 & \sqrt{\frac{3}{2}}B_\perp e^{i\phi} & 0 \\ 0 & 0 & \sqrt{\frac{3}{2}}B_\perp e^{-i\phi} & -B_z & B_\perp e^{i\phi} \\ 0 & 0 & 0 & B_\perp e^{-i\phi} & -2B_z \end{pmatrix}, \tag{2.29}$$

where we have assumed that the magnetic field is of the form

$$\mathbf{B} = \begin{pmatrix} B_\perp(r,z)\cos(\phi) \\ -B_\perp(r,z)\sin(\phi) \\ B_z(r,z) \end{pmatrix}. \tag{2.30}$$

The eigenvectors of $\mathcal{B}$ having positive eigenvalues are referred as WFSSs, zero eigenvalue as NS and negative eigenvalues as SFSSs. In particular, the WFSS_2 and WFSS_1 (SFSS_2 and SFSS_1) correspond to the eigenvalues $\mu_{\rm B}$ and $\mu_{\rm B}/2$ ($-\mu_{\rm B}$ and $-\mu_{\rm B}/2$), respectively.

The eigenvector for WFSS_2 turns out to be

$$\mathbf{w}_2 = \begin{pmatrix} \cos^4(\beta/2) \\ 2e^{i\phi}\cos^3(\beta/2)\sin(\beta/2) \\ \sqrt{6}e^{2i\phi}\cos^2(\beta/2)\sin^2(\beta/2) \\ 2e^{3i\phi}\cos(\beta/2)\sin^3(\beta/2) \\ e^{4i\phi}\sin^4(\beta/2) \end{pmatrix}, \tag{2.31}$$

where $\beta = \tan^{-1}(|B_\perp|/|B_z|)$ is the angle between the magnetic field and the z axis. By fixing the spin and phase degrees of freedoms to $\mathbf{w}_2$, the GP equation (2.27) for the spatial part of the order parameter $f(\mathbf{r})$ is obtained as

$$\mu f(\mathbf{r}) = -\frac{\hbar^2}{2m}\mathbf{w}_2^\dagger \nabla^2 (f\mathbf{w}_2) + V_{opt}(\mathbf{r})f(\mathbf{r}) + (g_1 + 4g_2)f^3(\mathbf{r}) + \hbar\omega_\mathrm{L} f(\mathbf{r}), \tag{2.32}$$

where the absolute value of the Larmor frequency $\omega_\mathrm{L} = \mu_\mathrm{B}|\mathbf{B}|$.

The topological method to create a multiquantum vortex may be understood directly from Eq. (2.31). Let us consider a setup in which the radial part of the magnetic field $B_\perp$ vanishes and the WFSS_2 is an eigenstate of F_z, *i.e.*, all the spins of the atoms are pointing in the direction of the magnetic field. While the magnetic field is being reversed adiabatically, the state remains in the WFSS_2 presented by Eq. (2.31) and, finally, when the field points exactly towards the negative z direction, the phase factor $e^{i4\phi}$, has been added to the order parameter. In the case of the hyperfine spin $F = 1$, the added phase factor is $e^{i2\phi}$, see Paper I.

The reversing of the magnetic field can be accomplished by holding the perpendicular field zero, which is not efficient, since spin flips to other spin states may occur anywhere in space when the field B_z vanishes. However, the region of the spin flips may be reduced to the z axis, if a finite $B_\perp$ is considered. The case $F = 1$ was studied in Refs. [71, 72], in which the optical potential was chosen to mimic a tightly focused blue-detuned laser beam in the center of the magnetic trap. The strength of the potential was high enough for the particles to be repelled from the center and, hence, the temporal evolution of the system was determined by the GP equation for the WFSS obtained, to a good approximation, using Eq. (2.32) with the replacement $\mu \to i\hbar\partial_t$. Naturally, the order parameter obtained contained a vortex according to our definition, but strictly speaking there was only a persistent current rather than a vortex, since there were no particles near the phase singularity. In Paper II, the use of an optical plug for the hyperfine spin $F = 2$ was studied. The temporal evolution of the total particle density is shown in Fig. 2.3 which illustrates how the position of the peak particle density is shifted towards the origin when the magnetic potential becomes steeper with decreasing magnitude of the B_z field.

In Paper II, removal of the optical plug after the vortex creation is demonstrated. After the removal, some oscillatory modes are seen in the condensate density. These oscillations arise from non-adiabatic changes in the optical potential and could be decreased by reducing the speed of the field removal. In the physical realizations, the finite

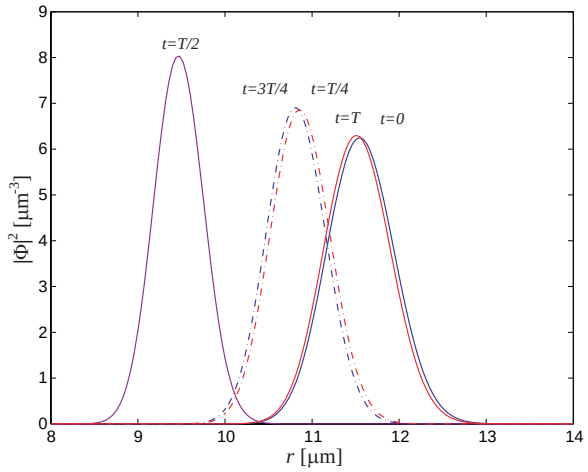

Figure 2.3: (color online) Temporal evolution of the total particle density as the bias field B_z is being reversed during the topological vortex formation. The reversing time is denoted by T.

lifetime of the condensate restricts the removal time such that at least small oscillations should remain. In Paper I, the topological creation of vortices in BECs with hyperfine spin $F = 1$ was studied without the use of the optical plug.

After the publication of Papers I and II, the experimental realization of the topological vortex-formation scenario seemed to be promising since the theory was developed for the already realized BECs in a Ioffe-Pritchard trap, in which the reversing of the magnetic field may be realized by reversing the electrical current in the coils creating the field B_z. However, the inclusion of the optical plug would have demanded additional apparata and refinements. In Papers I–II, the full spin degrees of freedom were taken into account and it was shown that the vortex can actually be created even in the absence of the optical potential. In this setup, the reversing time T was adjusted such that roughly only one half of the particles escaped from the trap due to spin flips to the NS and the SFSSs. For the hyperfine spin $F = 1$, the method resulted in a doubly quantized vortex state, see Paper I. On the other hand, both of the two WFSSs of the $F = 2$ condensate are trapped and the topological vortex formation produces a mixture of three- and fourfold quantized vortices. In Fig. 2.4, square roots of the particle densities for the WFSS_1 and the WFSS_2 are shown after the particles in the NS and the SFSSs have escaped from the trap. Since both of the trapped spinor states contain a noticeable fraction of the particles, the state cannot be considered a scalar condensate with a given vorticity.

2.4 Splitting of a doubly quantized vortex

Soon after the theoretical work on topological vortex formation without the optical plug was published, Leanhardt *et al.* reported on experimental realizations of two- and fourfold

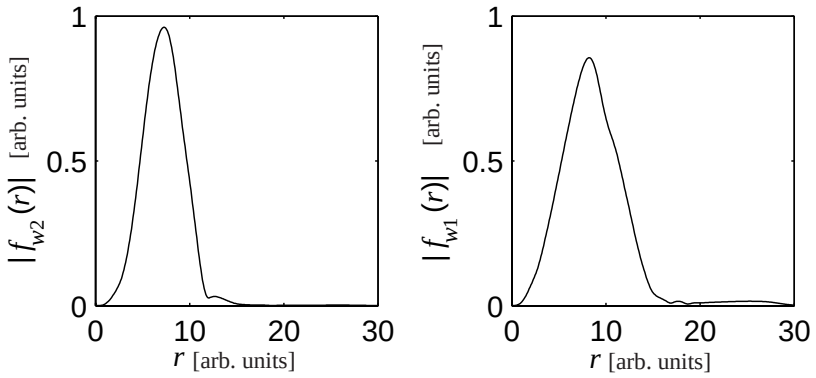

Figure 2.4: Amplitudes of the projection of the order parameter to the (a) WFSS_2 and (b) WFSS_1 after the untrapped components have escaped from the trap. Due to topological phase imprinting, the WFSS_2 (WFSS_1) has the phase winding 8π (6π) about the z-axis.

quantized vortices using this technique [73]. They employed the hyperfine spin states $F = 1$ and $F = 2$ of ^{23}Na atoms and measured the angular momentum per particle to be approximately $2\hbar$ for $F = 1$ and $4\hbar$ for $F = 2$. The multiply charged vortices were held in the trap for up to 20 ms and the states were not observed to decay.

The experiments [73] raised two important questions: why was the angular momentum per particle measured to be $(-4.4\pm0.4)\hbar$, whereas the theory predicts a value below $4\hbar$, and why are the multiply charged vortices not observed to split into singly quantized ones although they should be dynamically unstable? While the first question remains unanswered, the latter puzzle is investigated in this subsection following Paper II.

In Sec. 2.2, it was stated that the energy of the vortex dipole must be a decreasing function of the vortex separation d_2 for small enough d_2, i.e., the force arising from the interactions between the vortices points towards the center of the system in the limit $d_2 \to 0$. For two vortices a and b far apart in a homogeneous BEC, the transformation $\kappa_a \to -\kappa_a$ reverses the sign of the interaction force between the vortices. One thus expects the attraction of the vortex dipole to change into a repulsion of a vortex pair. Another indication of the energetical instability of a doubly quantized vortex is obtained by calculating the average kinetic energy $\langle T \rangle$ of the state representing a straight vortex line $\Phi(\mathbf{r}) = \sqrt{n_{\mathrm{c}}(r,z)}e^{i\kappa_\theta \phi}$ in the center of condensate. One obtains

$$\int \Phi^* \left(-\frac{\hbar^2\nabla^2}{2m}\right) \Phi \, d\mathbf{r} = \frac{\hbar^2}{2m} \int \left\{ \sqrt{n_{\mathrm{c}}} \left(\partial_r^2 + \frac{1}{r}\partial_r + \partial_z^2\right) \sqrt{n_{\mathrm{c}}} + \frac{n_{\mathrm{c}}\kappa^2}{r^2} \right\} d\mathbf{r}. \qquad (2.33)$$

The last term in this equation is quadratic in the quantum number κ, which suggests that vortices with multiple charge are energetically less favourable than the singly quantized ones. Actually, this is the reason why a vortex lattice [70] rather than a multiquantum vortex is observed in rapidly rotating harmonically trapped condensates. The above

arguments may be misleading since they do not properly take into account the modifications in energy due to density modulations of the condensate and the trapping potential. However, the solution of the Bogoliubov equations shows that the doubly quantized vortex is not only energetically unstable, but it may also be dynamically unstable. The imaginary part of the complex-frequency mode responsible for this dynamical instability is shown in Fig. 2.5 as a function of the interaction strength $an_z(z) = a\int \Phi(\mathbf{r})dxdy$ for a condensate being homogeneous in the z direction. These results, originally discovered in Ref. [74], yield the initial decay rate of the state.

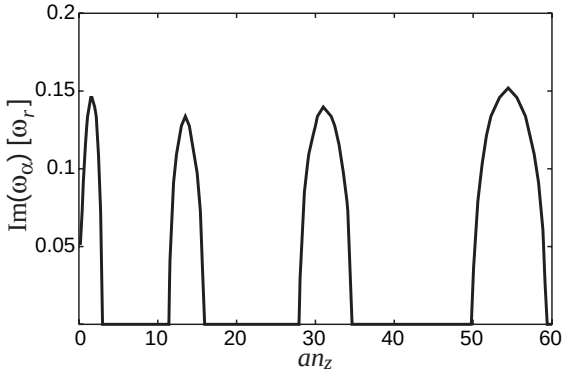

Figure 2.5: Imaginary part of the complex-frequency mode responsible for the dynamical instability of a doubly quantized vortex state is shown as a function of the interaction strength $an_z = a\int \Phi(\mathbf{r})dxdy$ for a condensate being homogeneous along the z direction.

In Paper III, the full dynamics of the decay of doubly quantized vortices is studied in the homogeneous and inhomogeneous cases. Let us consider a cigar-shaped condensate, for which the linear density $an_z(z)$ is z-dependent. The linear density vanishes at the tips of the cigar which correspond to the first instability region of the homogeneous case in Fig. 2.5. Provided that $an_z(0) \lesssim 11$, there are no other instability regions and the splitting of the vortex is expected to begin from the ends of the condensate. This analogy with the homogeneous situation has been verified by solving the temporal evolution of the system using the fully three-dimensional GP equation and by solving the Bogoliubov equations, for which the amplitude of the mode corresponding to the complex eigenvalue was localized mainly near the ends of the BEC. Figure 2.6 displays these results for the case of two splitting domains; $an_z(0) \approx 13$. The linear density $an_z(z)$ is shown in Fig. 2.6(a), in which the regions with a thick line represent values of an_z for which the homogeneous system is dynamically unstable. The modes with the highest imaginary frequencies, shown in Fig. 2.6(b), are localized mainly in these regions, *i.e.*, the splitting of the doubly quantized vortex is expected to start from the ends and also at the center of the condensate. Figure 2.6(c) justifies this prediction by showing the isosurfaces of the particle density at $t = 18.1$ ms and 41.4 ms after a sudden change in

the trap asymmetry $\omega_x/\omega_y : 1 \rightarrow 1.01$. The asymmetry triggers the splitting mechanism in the regions of the complex-frequency modes. The splitting is faster at the ends of the condensate, consistent with the fact that the modes concentrated in this region possess larger imaginary parts of the frequency than the other modes.

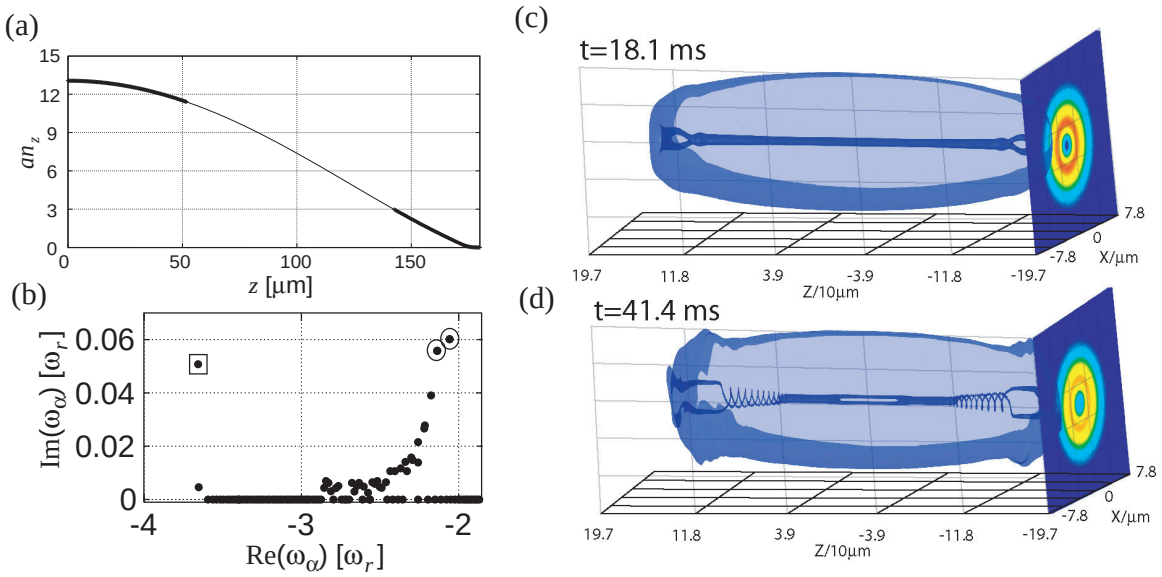

Figure 2.6: (color online) (a) Linear density an_z as a function of the z coordinate. The regions marked with a thick line represent values of an_z for which the homogeneous system is dynamically unstable. (b) Imaginary part of the excitation spectrum. The mode marked with the square is concentrated in the center of the condensate and the modes marked with circles at the ends. (c) Isosurfaces of the particle density of the condensate and the z-integrated particle densities at $t = 18.1$ ms and $t = 41.4$ ms after the sudden change in the trap asymmetry $\omega_x/\omega_y : 1 \rightarrow 1.01$.

As shown in Fig. 2.6(c), the two vortices intertwine as they split. This phenomenon is due to the fact that the precession frequency of a straight vortex pair arising from the repulsive interaction between the vortices depends on their distance. Since the distance is zero in the regions where the splitting has not yet began and finite in the other regions, it is necessary for the vortices to intertwine. The intertwining is observed to be quite strong and therefore it is difficult to detect the splitting only from the z-integrated particle densities shown in Figs. 2.6(c) and 2.6(d). Naturally, the regions where the splitting has not yet began also affect the average particle density in a similar way.

In Ref. [75], the splitting of a doubly quantized vortex was experimentally studied in ^{23}Na condensates for the hyperfine spin state $F = 1$. The vortex was created using the topological vortex formation and the system was let to evolve for the time τ_{h}, after which

the z-integrated particle density was measured. The particle densities indicated whether the vortex had split or not. This process was carried out with several hold times $\tau_{\rm h}$ and particle numbers and the result was that the shortest time $\tau_{\rm c}$ for which the splitting is observed became a monotonically increasing function of the particle number. This behaviour is consistent with the theoretical studies of Paper III*, since as the maximum linear density rises from value 4 to 11, the fraction of the particles in the regions where the splitting mechanism is very slow also increases. This phenomenon is seen as an effective increase of the vortex lifetime, when it is determined on the basis of the z-integrated particle density. The existence of the second peak in Fig. 2.5 is observed as the decrease in the derivative of $\tau_{\rm c}$ with respect to the maximum linear density for $an_z(0) \gtrsim 11$. This analysis of the resuls of Ref. [75] has not been published previously.

*The analysis in Ref. [75] may give an impression that the experimental results cannot be understood using the results of Paper III. Calculations which fit the exact experimental setup are being executed and the results will be published in future.

3 Finite-Temperature Mean-Field Theories

This section is devoted to the presentation of the finite-temperature second order theory for excitations in partially condensed alkali atom gases developed by Morgan *et al.* [50, 51, 59]. This theory utilizes systematic perturbation theory to take into account the interaction terms in the Hamiltonian. The extension of the theory presented in Refs. [57, 58], also takes into account external time-dependent perturbations of the system, but this is beyond the scope of this overview. Following Refs. [50,51] and Paper V, we present the so-called zeroth, first and second order theories in Secs. 3.1 and 3.2. In Sec. 3.3, we utilize the second order theory to investigate the energies and decay of the excitations in a pancake-shaped BEC.

3.1 Zeroth order theory

The starting point is the usual second-quantized Hamiltonian for structureless bosons

$$\hat{H} = \sum_{ij} \langle i|\hat{h}|j\rangle \hat{a}_i^\dagger \hat{a}_j + \frac{1}{2} \sum_{ijkm} \langle ij|V|km\rangle \hat{a}_i^\dagger \hat{a}_j^\dagger \hat{a}_k \hat{a}_m, \tag{3.1}$$

where the creation and annihilation operators $a_i^\dagger$ and a_i, as well as the single-particle Hamiltonian $\hat{h}$ and the interparticle potential V, were introduced in Sec. 2.1. We choose to employ the canonical ensemble with a fixed total number of particles N. Note that in the finite-temperature theory the total number of particles is expressed as the sum of the condensed and the excited particles as $N = N_\mathrm{c} + N_\mathrm{ex}$, whereas in the zero-temperature theory of Sec. 2, the number of the thermal particles was approximated to vanish. Since the state $|0\rangle$ is considered to be the condensate state, N_c is also referred as N_0. The operators for the particle numbers are given by $\hat{N}_0 = \hat{a}_0^\dagger \hat{a}_0$ for the condensate state and $\hat{N}_\mathrm{ex} = \sum_{k=1}^{\infty} \hat{a}_k^\dagger \hat{a}_k$ for the excited states.

By defining the bosonic number-conserving operators $\hat{\alpha}_i = [(\hat{N}_0 + 1)^{-1/2} \hat{a}_0]^\dagger \hat{a}_i$, one can decompose the Hamiltonian (3.1) as follows:

$$\hat{H} = \sum_{i=0}^{4} \hat{H}_i + O(N_0[\hat{\delta}/N_0]^{5/2}), \tag{3.2}$$

where

$$\hat{H}_0 = N_0 \left[\langle 0|\hat{h}|0\rangle + \frac{1}{2} N_0 \langle 00|V^{\rm s}|00\rangle \right], \tag{3.3}$$

$$\hat{H}_1 = \sqrt{N_0} \sum_{i\neq 0} \left[\langle i|\hat{h}|0\rangle + N_0 \langle i0|V^{\rm s}|00\rangle \right] \hat{\alpha}_i^\dagger + \text{h.c.}, \tag{3.4}$$

$$\hat{H}_2 = \sum_{ij\neq 0} \left[\langle i|\hat{h}|j\rangle - \mu\delta_{ij} + 2N_0 \langle 0i|V^{\rm s}|j0\rangle \right] \hat{\alpha}_i^\dagger \hat{\alpha}_j + \sum_{ij\neq 0} \left[\frac{N_0}{2} \langle ij|V^{\rm s}|00\rangle \hat{\alpha}_i^\dagger \hat{\alpha}_j^\dagger + \text{h.c.} \right] + \mu \langle \hat{N}_{\rm ex}\rangle, \tag{3.5}$$

$$\hat{H}_3 = \sum_{ijk\neq 0} \left[\sqrt{N_0} \langle ij|V^{\rm s}|k0\rangle \hat{\alpha}_i^\dagger \hat{\alpha}_j^\dagger \hat{\alpha}_k + \text{h.c.} \right], \tag{3.6}$$

$$\hat{H}_4 = \sum_{ijkm\neq 0} \frac{1}{2} \langle ij|V^{\rm s}|km\rangle \hat{\alpha}_i^\dagger \hat{\alpha}_j^\dagger \hat{\alpha}_k \hat{\alpha}_m, \tag{3.7}$$

and $\hat{\delta} = \hat{N}_{\rm ex} - \langle \hat{N}_{\rm ex}\rangle$ is the number fluctuation operator of the noncondensate particles. The symmetrized matrix elements of the two-particle interaction potential $V(\mathbf{r})$ are defined as

$$\langle ij|V^{\rm s}|km\rangle = \frac{1}{2}[\langle ij|V|km\rangle + \langle ji|V|km\rangle],$$

and μ as

$$\mu = \langle 0|\hat{h}|0\rangle + N_0 \langle 00|V^{\rm s}|00\rangle,$$

where the average number of atoms in the condensate state is given by $N_0 = N - \langle \hat{N}_{\rm ex}\rangle$. In the above equations, the averages $\langle \ldots \rangle$ refer to quantum expectation values and h.c. stands for hermitian conjugate.

In the zeroth order approximation, one solves the ground state $|0\rangle$ of $\hat{H}_0$ alone, which makes the linear Hamiltonian $\hat{H}_1$ to vanish. The equation for the ground state in the coordinate space becomes the GP equation (2.12), but in the notation of this section we use an orthonormal single-particle basis $\zeta_i(\mathbf{r}) = \langle \mathbf{r}|i\rangle$ and, thus, we have to make the substitution $\Phi(\mathbf{r}) = \sqrt{N_0}\zeta_0(\mathbf{r})$ into Eq. (2.12). To diagonalize $\hat{H}_2$, we employ the Bogoliubov transformation $\hat{\beta}_i = \sum_{j\neq 0} \left(U_{ij}^* \hat{\alpha}_j - V_{ij}^* \hat{\alpha}_j^\dagger \right)$. This results in the Bogoliubov equations (2.16), in which the quasiparticle amplitudes are related to the transformation by $u_i(\mathbf{r}) = \sum_{j\neq 0} U_{ij}\zeta_j(\mathbf{r})$ and $v_i(\mathbf{r}) = \sum_{j\neq 0} V_{ij}\zeta_j^*(\mathbf{r})$. One should note that the Bogoliubov equations have the zero-energy solution $\{u_0(\mathbf{r}), v_0(\mathbf{r})\} = \{\zeta_0(\mathbf{r}), -\zeta_0^*(\mathbf{r})\}$, and projection to this homogeneous solution should always be subtracted from the quasiparticle amplitudes.

To calculate the lowest-order mean fields, i.e., the density of the thermal atoms $\rho(\mathbf{r}) = \sum_{ij\neq 0} \zeta_j^*(\mathbf{r})\zeta_i(\mathbf{r})\langle \hat{\alpha}_j^\dagger \hat{\alpha}_i\rangle$ and the so-called anomalous average $\kappa(\mathbf{r}) = \sum_{ij\neq 0} \zeta_j(\mathbf{r})\zeta_i(\mathbf{r})\langle \hat{\alpha}_j \hat{\alpha}_i\rangle$,

we express the particle operators in terms of quasiparticle operators, yielding

$$\rho(\mathbf{r}) = \sum_{i\neq 0} \left[(|u_i(\mathbf{r})|^2 + |v_i(\mathbf{r})|^2) n_i + |v_i(\mathbf{r})|^2 \right], \tag{3.8}$$

$$\kappa(\mathbf{r}) = \sum_{i\neq 0} u_i(\mathbf{r}) v_i^*(\mathbf{r})(2n_i + 1). \tag{3.9}$$

In principle, the quasiparticle populations $n_i = \langle \hat{\beta}_i^\dagger \hat{\beta}_i \rangle$ should be calculated from the requirement that the canonical partition function $\mathcal{Z}_\mathrm{c} = \sum_{\{n_i\}} e^{-\beta E_i(\{n_i\})}$ minimizes the free energy $\mathcal{F} = -k_\mathrm{B} T \log \mathcal{Z}_\mathrm{c}$. However, to a fair approximation [90] one may use the non-interacting quasiparticle gas result $n_i = (z^{-1} e^{\beta\varepsilon_i} - 1)^{-1}$, where the fugacity is calculated from the relation $z = N_0/(1 + N_0)$. The effective delta-function potential used as the interparticle potential in this overview is inapplicable at high energies and leads to an ultraviolet divergence in the anomalous average which has to be renormalized in a proper way, see Paper V.

In this zeroth order theory, we solve the GP equation for some N_0, after which we compute the excitation spectrum and the number of the excited particles $N_\mathrm{ex} = \int \rho(\mathbf{r}) d\mathbf{r}$. This process must be iterated to find such an N_0 that the total number of particles satisfies $N = N_0 + N_\mathrm{ex}$. Thus the only contribution of the thermal gas to the excitation energies and the condensate is through the change in the number of the condensed particles. This zeroth order theory does not converge to the one used in Sec. 2 in the limit $T \to 0$ since the thermal particle density has a temperature-independent term. This residual fraction of the particles arises directly from the atomic interactions.

3.2 First and second order theories

In calculating the perturbative corrections to the zeroth order theory corresponding to Eqs. (2.12) and (2.16), it is convenient to first calculate the improved condensate wave function $\tilde{\zeta}_0(\mathbf{r})$ from the generalized Gross-Pitaevskii (GGP) equation

$$\left[-\frac{\hbar^2}{2m}\nabla^2 + V_\mathrm{trap}(\mathbf{r}) + N_0 g |\tilde{\zeta}_0(\mathbf{r})|^2 + 2g\rho(\mathbf{r}) \right] \tilde{\zeta}_0(\mathbf{r}) + U_0 \kappa(\mathbf{r}) \tilde{\zeta}_0^*(\mathbf{r}) = \mu_\mathrm{g} \tilde{\zeta}_0(\mathbf{r}), \tag{3.10}$$

which is obtained by minimizing $\langle \hat{H}_0 \rangle + \langle \hat{H}_2 \rangle$. Expressing the terms in the Hamiltonian as

$$\hat{H}_i[\tilde{\zeta}_0] = \hat{H}_i[\zeta_0] + \Delta\hat{H}_i, \tag{3.11}$$

one finds the perturbative Hamiltonian

$$\hat{H}_\mathrm{pert} = \Delta\hat{H}_0 + \Delta\hat{H}_1 + \Delta\hat{H}_2 + \hat{H}_3 + \hat{H}_4, \tag{3.12}$$

where the non-quadratic terms $\hat{H}_3$ and $\hat{H}_4$ are to be calculated using the improved condensate wave function.

The perturbation term $\Delta\hat{H}_0$ is just a real number and can easily be taken into account. In addition to it, in the first order perturbation theory only the terms $\Delta\hat{H}_2$ and $\hat{H}_4$ containing even numbers of quasiparticle operators contribute to the energy shift

$$E_{\rm pert}(s,1) = \langle s|\hat{H}_{\rm pert}|s\rangle, \tag{3.13}$$

where $|s\rangle$ is an eigenstate of the quasiparticle occupation number. Within the second order perturbation theory, one can in fact neglect the terms $\Delta\hat{H}_2$ and $\hat{H}_4$ since it turns out that their contributions are of the same order of magnitude as the contribution of the other terms in the third order perturbation theory [50, 51]. Thus, one only needs to calculate

$$E_{\rm pert}(s,2) = \sum_{r\neq s} \frac{|\langle r|\Delta\hat{H}_1 + \hat{H}_3|s\rangle|^2}{E_s - E_r}. \tag{3.14}$$

The quasiparticle energies are calculated as total energy changes of the system when the corresponding quasiparticle occupation number is increased by one while the total number of particles is held constant, *i.e.*, $E_p = E(N_0 - \Delta N_p, n_1, n_2, \ldots, n_p + 1, \ldots) - E(N_0, n_1, n_2, \ldots)$, where $\Delta N_p = \int {\rm d}\mathbf{r}[|u_p(\mathbf{r})|^2 + |v_p(\mathbf{r})|^2]$ is the amount of particles transferred to the mode p. This yields the corrected excitation energy

$$E_p(z') = \varepsilon_p + \Delta E_4^p + \Delta E_{\rm shape}^p + \Delta E_\mu^p + \Delta E_3^p(z'), \tag{3.15}$$

where the Δ-terms are given in Paper V and the complex energy parameter z' should not be confused with the fugacity. The need to compute the quasiparticle energies as functions of z' is naturally related with the fact that one takes into account quasiparticle interactions, though only to the lowest order, and the quasiparticle states are no more energy eigenstates having infinite lifetimes. In addition, in computing the quasiparticle energies z' must have a small imaginary part acting as a regularizer for the otherwise divergent expressions for the second order energy shifts. One may note that setting $z' = \varepsilon_p$ yields the usual Rayleigh-Schrödinger perturbation theory, while the Brillouin-Wigner perturbation theory corresponds to solving the equation $E_p(z') = z'$.

Calculating the excitation energies as functions of z' yields the dynamics of the excitations in the following way: The time-evolution operator $\hat{U}(t)$ of the system may be written in terms of the Fourier transform of the resolvent operator $\hat{G}(z') = (z' - \hat{H})^{-1}$ as [91]

$$\hat{U}(t) = -\frac{\hbar}{\pi}\int_{-\infty}^{\infty} e^{-i\omega t}{\rm Im}[\hat{G}(\hbar\omega - i0)]d\omega. \tag{3.16}$$

Let us define the projection of the resolvent to the state p as $G_p(z) = \langle p|\hat{G}|p\rangle$, which may be approximated to the second order as

$$G_p(\omega) = [\hbar\omega - E_p(\hbar\omega)]^{-1}. \tag{3.17}$$

Finally, it is seen that the imaginary part of the projected resolvent $F_p(\omega - i0) = {\rm Im}[G_p(\omega - i0)]$ gives the spectral distribution of the mode p and the Fourier transform of $F_p(\omega)$ yields its time dependence.

In conclusion, the second order theory may be used to calculate the energies and the dynamics of the quasiparticles. First the GP equation (2.12) is solved together with the Bogoliubov equations (2.16) for a given total particle number $N = N_0 + N_{\rm ex}$. Then the GGP equation (3.10) is solved, after which the spectrum $F_p(\omega)$ may be extracted for each excitation p using the energy corrections in Eq. (3.15). In addition, one has to take care of proper ultraviolet renormalization in all calculations; the quantities $\kappa(\mathbf{r})$ and ΔE_3^p are to be replaced by their renormalized values given in Paper V.

A first order theory is obtained from the second order theory by only taking the correction terms from the first order perturbation theory. However, the equations obtained turn out to match with those of the HFB theory which is known to display an energy gap in the spectrum in the homogeneous limit. This energy gap introduces an anomalous dependence of the lowest-energy modes on the trapping frequency. The simplest gapless theory known is the HFB-Popov theory [40, 41] obtained by neglecting the anomalous correlation. Thus, a useful first order theory is obtained from the second order theory by putting $\kappa(\mathbf{r})$ and $\Delta E_3^p(z')$ equal to zero by hand. The omission of the computationally awkward second order correction renders the first order theory to be computationally more convenient than the second order theory.

3.3 Energies and decay of excitations

In this section we consider a BEC of $N = 2000$ ^{23}Na particles in a pancake-shaped trap for which $\omega_r \ll \omega_z$. The trapping frequency in the tight direction is chosen to be $\omega_z = 2\pi \times 350$ Hz. The z-dependence of the order parameter may be taken to be of the Gaussian form $\sigma_z(z) = e^{-z^2/(2a_z^2)}/\sqrt{a_z\pi^{1/2}}$ and the harmonic oscillator lengths of the trap are $a_i = \sqrt{\hbar/m\omega_i}$. It turns out that by measuring length in units of a_r and the time in ω_r^{-1}, the GP equation for the system (2.19) becomes independent of the radial trapping frequency ω_r. Hence, the computed results apply for any physical value of ω_r with the restriction $\omega_r \ll \omega_z$.

The fraction of the condensed particles is plotted in Fig. 3.1, from which we identify the condensation temperature $T_{\rm BEC}$ as the point at which the condensate fraction obtains its maximum second derivative with respect to temperature. The energies of the low-lying modes are presented as functions of temperature in Fig. 3.2 in which the angular-momentum quantum numbers of the modes in the order of increasing energy are $q_\theta = 1$, 2, 0, and 1, which correspond to quanta of $\hbar$ in the angular momentum per particle. The mean values of the spectral distributions of the excitation energies within the second order theory are shown, in addition to the corresponding HFB-Popov results. The second order theory is probably not reliable above or in the vicinity of $T_{\rm BEC}$, although we present its predictions also in this regime. No systematic behaviour of the second order corrections is seen in Fig. 3.2. For the high-lying modes, however, it is reported in Paper V that the second order theory yields systematically larger energies compared with the HFB-Popov results.

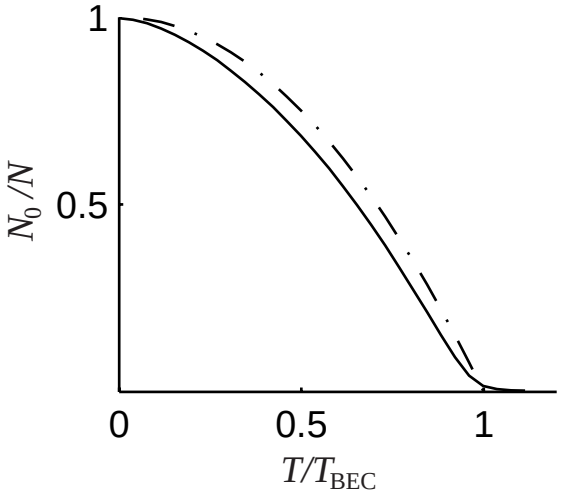

Figure 3.1: Condensate fraction as a function of temperature (solid line), and the exact result $1-(T/T_{\mathrm{BEC}})^2$ for the non-interacting system (dashed-dotted line).

In Fig. 3.2, the dashed line corresponds to the energy $\hbar\omega_r$ of the exact center-of-mass oscillation modes, the Kohn modes. According to the generalization [92, 93] of Kohn's theorem [94], a system of harmonically trapped interacting particles in any eigenstate of the Hamiltonian has an eigenstate with the amount $\hbar\omega_i$ higher energy, i.e., the exact diagonalization of the Hamiltonian should yield a spectrum that contains the eigenenergy $\hbar\omega_i$. The Bogoliubov theory, in which the thermal gas component is neglected, implies the Kohn modes to have this exact energy. In the higher-order theories, the mean fields and their interactions with the condensate are to be taken into account in such a way that the results are consistent with the Kohn theorem. Figure 3.2 shows that within the second order theory the energy of the Kohn mode is very close to $\hbar\omega_r$ for temperatures $T < 0.8T_{\mathrm{BEC}}$. Taking into account perturbation-theoretical terms beyond the second order contributions, energies even closer to the exact result should be obtained.

The lowest mode with vanishing angular momentum is the breathing mode, corresponding to uniform scaling oscillations of the condensate. In the case of a two-dimensional harmonically trapped gas interacting via the contact potential, it has been shown using the scaling symmetry of the Hamiltonian that there exists a state that has the energy $2\hbar\omega_r$ in excess to that of the ground state [95]. This excitation is identified as the breathing mode. The Bogoliubov theory yields exactly the energy $2\hbar\omega_r$ for the breathing mode, while the Popov and the second order theories do not, as can be seen in Fig. 3.2. Since the interaction potential has to be renormalized and, hence, it deviates from the contact potential used in Ref. [95] for modes with high energy, the applicability of the exact result is somewhat questionable at high temperatures, where the physics is

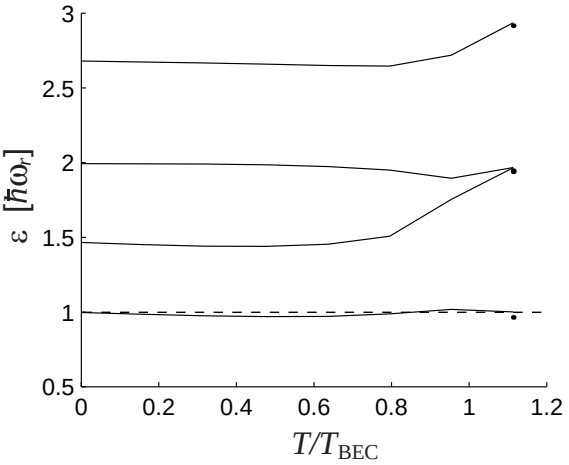

Figure 3.2: Temperature dependence of the mean energies of low-lying modes corresponding to the angular-momentum quantum numbers $q_\theta = 1$, 2, 0, and 1, in the order of increasing energy. Dots correspond to the second order theory, and the solid lines to the HFB-Popov theory. The dashed line indicates the exact energy $\hbar\omega_r$ of the Kohn modes.

not determined by the low-lying modes alone. It is shown in Fig. 3.2 that the energy of the breathing mode is lower than $2\hbar\omega_r$ and the deviation increases with temperature.

In experiments and theoretical studies, the decay of excitations is commonly characterized only by the damping rate related to the exponential decay of the oscillation amplitude. For infinite systems, the excitation spectrum is continuous and the spectral distributions $F_p(\omega)$ of the excitations have Lorentzian forms, implying indeed an exponential decay of the mode oscillations. The mean value of the Lorentzian gives the mode frequency and its width the damping rate. However, for trapped finite systems the spectrum is discrete and the spectral distributions generally have more complicated forms. Especially, the dynamics implied by these distributions can be more complicated than just the simple exponential decay. Using the computed spectral distributions of the oscillations, we have studied the validity of the exponential-decay approximation for the finite system under question.

The spectral distribution and the dynamics of the second lowest mode with the angular momentum quantum number $q_\theta = 1$ at the temperature $T = 0.64T_{\rm BEC}$ is shown in Fig. 3.3. The distribution is obviously far from Lorentzian form, consisting of several asymmetrically separated peaks. The collapse and revival behaviour is clearly seen when the amplitude of the oscillation seems to vanish but then grows again in time. In Paper V, a strong collapse and revival of the breathing mode was also studied but, in that case, the phenomenon may be an artefact of the second order theory arising from the accidentally

resonant Beliaev process between the Breathing and the Kohn modes. Nevertheless, our calculations have showed collapse and revival of many elementary excitations for which the resonance has no effect.

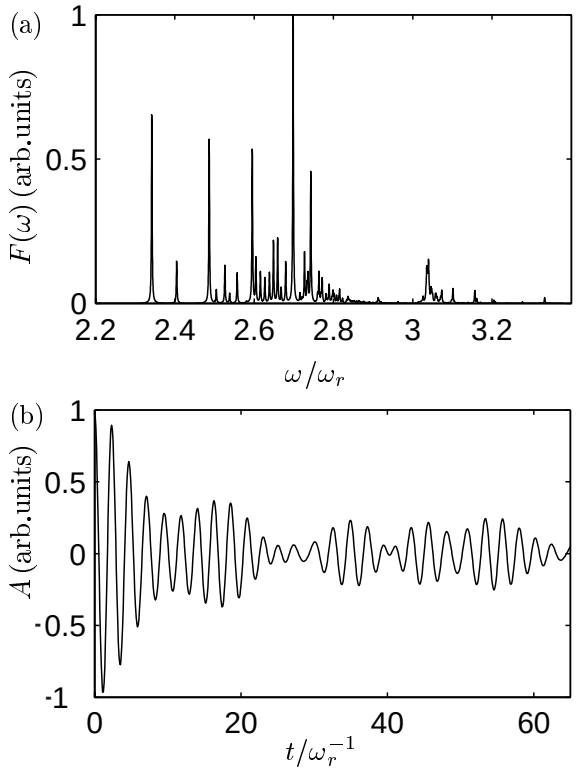

Figure 3.3: (a) Spectral distribution $F(\omega)$ of the second lowest mode with the angular momentum $\hbar$ per particle and (b) its Fourier transform at the temperature $T = 0.64 T_{\mathrm{BEC}}$.

In conclusion, we have studied the temperature dependence of the excitation energies of the ground state in a pancake-shaped BEC. This, as well as the observation of the collapse and revival effect within the second order theory was first accomplished in Paper V. In addition, a comparison of the second order theory with the exact results for the Kohn and the breathing modes has not been carried out in the literature prior to Paper V.

4 Summary

The main objective of this thesis is to study vortices and elementary excitations in dilute atomic Bose-Einstein condensates.

In Papers I–II, the topological phase imprinting method was simplified in order to make it more accessible to the experiments. In this method, the condensate atoms are in a WFSS and trapped in a Ioffe-Pritchard magnetic trap. To create the vortex, the electrical current producing the bias magnetic field is reversed. Soon after the publication of these results, the first two- and fourfold quantized vortices were produced by the MIT group.

In the theoretical investigations of Papers I–II, it was observed that whereas the topologically created doubly quantized vortex is pure, the fourfold quantized vortex state is actually a mixture of angular momenta $4\hbar$ and $3\hbar$ per particle. Therefore, the doubly quantized vortex was chosen as the topic of Paper III, in which the dynamics of the splitting of the vortex into two singly quantized vortices was modelled in a cigar-shaped trap. The main result of the paper was the finding that there exists a close analogy between the effectively two-dimensional and the true dynamics of the splitting. The two singly quantized vortices were observed to intertwine as they separate, which implies the observation of the splitting to be more favourable in the transverse directions of the cigar compared with the longitudinal direction. Recently, the splitting of the doubly quantized vortex was observed by the MIT group and the results were in harmony with our theoretical predictions.

Stationary vortex clusters are considered in Paper IV. This work is an extension of earlier work, in which the existence of complex clusters was shown in the non-interacting limit and the dynamical stability of the vortex dipole and quadrupole was demonstrated in the interacting system. In our research, we showed explicitly that the vortex dipole and quadrupole obtained were, in fact, stationary to a very high precision. However, the states were found to be both dynamically and energetically unstable in terms of the Bogoliubov equations and the Gross-Pitaevskii equation. We also introduced a novel structure called a vortex tripole, a non-axisymmetric stationary state holding finite angular momentum in a non-rotating harmonic trap.

Paper V is devoted to the study of the previously developed second order theory for BECs at finite temperatures. This theory was applied for the first time to pancake-shaped condensates, for which the excitation energies and their decay was computed. Especially, the collapse and revival effects in the dynamics of the excitations was observed. In addition, the accuracy of the theory is tested by comparing its predictions to the exactly known results for the breathing mode and the Kohn modes.

In a nutshell, this thesis includes original, experimentally realized, theoretical results on the creation and stability of vortices in BECs. Furthermore, new results have been presented in the area of stationary vortex states. Although the study of the second order theory of excitations in BECs is presented in only a single paper, the work was

very demanding both theoretically and computationally. Possible new areas of research include further developing the topological formation of vortices, studying the dynamics of the spinor mixture state created in the MIT experiments, describing in detail the experiments on the splitting of the doubly quantized vortex, extending the stability analysis of vortex clusters to three-dimensional or anharmonically trapped structures, and applying the second order theory to the stability analysis of the singly quantized vortex.

References

[1] S. Bose, Z. Phys. **26**, 178 (1924).

[2] A. Einstein, Sitzungber. Kgl. Preuss. Akad. Wiss. **1924**, 261 (1924).

[3] A. Einstein, Sitzungber. Kgl. Preuss. Akad. Wiss. **1925**, 3 (1925).

[4] F. London, Phys. Rev. **54**, 947 (1938).

[5] F. London, Nature **141**, 643 (1938).

[6] P. Sokol, in *Bose-Einstein Condensation*, edited by A. Griffin, D. W. Snoke, and S. Stringari (Cambridge University Press, Cambridge, 1995), Chap. 4, pp. 51–85.

[7] D. M. Ceperley, Rev. Mod. Phys. **67**, 279 (1995).

[8] J. Bardeen, L. N. Cooper, and J. R. Schrieffer, Phys. Rev. **108**, 1175 (1957).

[9] S. Stenholm, Rev. Mod. Phys. **58**, 699 (1986).

[10] S. Chu, Rev. Mod. Phys. **70**, 685 (1998).

[11] C. N. Cohen-Tannoudji, Rev. Mod. Phys. **70**, 707 (1998).

[12] W. D. Phillips, Rev. Mod. Phys. **70**, 721 (1998).

[13] C. E. Wieman, D. E. Pritchard, and D. J. Wineland, Rev. Mod. Phys. **71**, S253 (1999).

[14] C. J. Pethick and H. Smith, *Bose-Einstein Condensation in Dilute Gases* (Cambridge University Press, Cambridge, 2002).

[15] L. Pitaevskii and S. Stringari, *Bose-Einstein Condensation* (Oxford University Press Inc., New York, 2003).

[16] W. Wing, Prog. Quantum Electron. **8**, 181 (1984).

[17] E. L. Raab, M. Prentiss, A. Cable, S. Chu, and D. E. Pritchard, Phys. Rev. Lett. **59**, 2631 (1987).

[18] M. H. Anderson, J. R. Ensher, M. R. Matthews, C. E. Wieman, and E. A. Cornell, Science **269**, 198 (1995).

[19] K. B. Davis, M.-O. Mewes, M. R. Andrews, N. J. van Druten, D. S. Durfee, D. M. Kurn, and W. Ketterle, Phys. Rev. Lett. **75**, 3969 (1995).

[20] C. C. Bradley, C. A. Sackett, J. J. Tollett, and R. G. Hulet, Phys. Rev. Lett. **75**, 1687 (1995), *ibid.* **79**, 1170 (1997).

[21] D. G. Fried, T. C. Killian, L. Willmann, D. Landhuis, S. C. Moss, D. Kleppner, and T. J. Greytak, Phys. Rev. Lett. **81**, 3811 (1998).

[22] S. L. Cornish, N. R. Claussen, J. L. Roberts, E. A. Cornell, and C. E. Wieman, Phys. Rev. Lett. **85**, 1795 (2000).

[23] F. P. D. Santos, J. Lonard, J. Wang, C. J. Barrelet, F. Perales, E. Rasel, C. S. Unnikrishnan, M. Leduc, and C. Cohen-Tannoudji, Phys. Rev. Lett. **86**, 3459 (2001).

[24] A. Robert, O. Sirjean, A. Browaeys, J. Poupard, S. Nowak, D. Boiron, C. I. Westbrook, and A. Aspect, Science **292**, 461 (2001).

[25] G. Modugno, G. Ferrari, G. Roati, R. J. Brecha, A. Simoni, and M. Inguscio, Science **294**, 1320 (2001).

[26] T. Weber, J. Herbig, M. Mark, H.-C. Nägerl, and R. Grimm, Science **299**, 232 (2002).

[27] M. Greiner, C. A. Regal, and D. S. Jin, Nature **426**, 537 (2003).

[28] S. Jochim, M. Bartenstein, A. Altmeyer, G. Hendl, S. Riedl, C. Chin, J. H. Denschlag, and R. Grimm, Science **302**, 2101 (2003).

[29] M. W. Zwierlein, C. A. Stan, C. H. Schunck, S. M. F. Raupach, S. Gupta, Z. Hadzibabic, and W. Ketterle, Phys. Rev. Lett. **91**, 250401 (2003).

[30] C. A. Regal, M. Greiner, and D. S. Jin, Phys. Rev. Lett. **92**, 40403 (2004).

[31] E. Tiesinga, B. J. Verhaar, and H. T. C. Stoof, Phys. Rev. A **47**, 4114 (1993).

[32] S. Inouye, M. R. Andrews, J. Stenger, H.-J. Miesner, D. M. Stamper-Kurn, and W. Ketterle, Nature **392**, 151 (1998).

[33] L. D. Landau and E. M. Lifshitz, *Quantum Mechanics - Non-Relativistic Theory* (Pergamon Press, Oxford, 1977).

[34] C. J. Joachain, *Quantum Collision Theory* (North Holland, Amsterdam, 1983).

[35] M. Le Bellac, *Thermal Field Theory* (Cambridge University Press, Cambridge, 1996).

[36] D. S. Jin, J. R. Ensher, M. R. Matthews, C. E. Wieman, and E. A. Cornell, Phys. Rev. Lett. **77**, 420 (1996).

[37] M.-O. Mewes, M. R. Andrews, N. J. van Druten, D. M. Kurn, D. S. Durfee, C. G. Townsend, and W. Ketterle, Phys. Rev. Lett. **77**, 988 (1996).

[38] M. Edwards, P. A. Ruprecht, K. Burnett, R. J. Dodd, and C. W. Clark, Phys. Rev. Lett. **77**, 1671 (1996).

[39] S. Stringari, Phys. Rev. Lett. **77**, 2360 (1996).

[40] V. N. Popov, in *Functional Integrals and Collective Modes* (Cambridge University Press, New York, 1987), Chap. 6.

[41] A. Griffin, Phys. Rev. B **53**, 9341 (1996).

[42] D. S. Jin, M. R. Matthews, J. R. Ensher, C. E. Wieman, and E. A. Cornell, Phys. Rev. Lett. **78**, 764 (1997).

[43] D. A. W. Hutchinson, R. J. Dodd, and K. Burnett, Phys. Rev. Lett. **81**, 2198 (1998).

[44] A. Minguzzi and M. P. Tosi, J. Phys.: Condens. Matter **9**, 10211 (1997).

[45] G. Bene and P. Szpfalusy, Phys. Rev. A **58**, R3391 (1998).

[46] P. O. Fedichev and G. V. Shlyapnikov, Phys. Rev. A **58**, 3146 (1998).

[47] M. Rusch and K. Burnett, Phys. Rev. A **59**, 3851 (1999).

[48] J. Reidl, A. Csordás, R. Graham, and P. Szépfalusy, Phys. Rev. A **61**, 43606 (2000).

[49] S. Giorgini, Phys. Rev. A **61**, 63615 (2000).

[50] S. Morgan, J. Phys. B: At. Mol. Opt. Phys. **33**, 3847 (2000).

[51] S. Morgan, Ph.D. thesis, University of Oxford, 2000.

[52] E. Zaremba, A. Griffin, and T. Nikuni, Phys. Rev. A **57**, 4695 (1998).

[53] T. Nikuni, E. Zaremba, and A. Griffin, Phys. Rev. Lett. **83**, 10 (1999).

[54] E. Zaremba, T. Nikuni, and A. Griffin, J. Low. Temp. Phys. **116**, 277 (1999).

[55] R. Walser, J. Williams, J. Cooper, and M. Holland, Phys. Rev. A **59**, 3878 (1999).

[56] N. P. Proukakis, J. Phys. B **34**, 4737 (2001).

[57] S. A. Morgan, M. Rusch, D. A. W. Hutchinson, and K. Burnett, Phys. Rev. Lett. **91**, 250403 (2003).

[58] S. A. Morgan, Phys. Rev. A **69**, 23609 (2004).

[59] M. Rusch, S. A. Morgan, D. A. W. Hutchinson, and K. Burnett, Phys. Rev. Lett. **85**, 4844 (2000).

[60] T. Mizushima, M. Ichioka, and K. Machida, Phys. Rev. Lett. **90**, 180401 (2003).

[61] O. M. Maragó, S. A. Hopkins, J. Arlt, E. Hodby, G. Heckenblaikner, and C. J. Foot, Phys. Rev. Lett. **84**, 2056 (2000).

[62] E. Hodby, O. M. Maragó, G. Heckenblaikner, and C. J. Foot, Phys. Rev. Lett. **86**, 2196 (2001).

[63] D. Cribier, B. Jacrot, C. M. Rao, and B. Forttoux, Phys. Lett. **9**, 106 (1964).

[64] G. A. Williams and R. E. Packard, Phys. Rev. Lett. **33**, 280 (1974).

[65] M. R. Matthews, B. P. Anderson, P. C. Haljan, D. S. Hall, C. E. Wieman, and E. A. Cornell, Phys. Rev. Lett. **83**, 2498 (1999).

[66] K. W. Madison, F. Chevy, W. Wohlleben, and J. Dalibard, Phys. Rev. Lett. **84**, 806 (2000).

[67] K. W. Madison, F. Chevy, W. Wohlleben, and J. Dalibard, J. Mod. Opt. **47**, 2715 (2000).

[68] C. Raman, J. R. Abo-Shaeer, J. M. Vogels, K. Xu, and W. Ketterle, Phys. Rev. Lett. **87**, 210402 (2001).

[69] E. Hodby, G. Heckenblaikner, S. A. Hopkins, O. M. Maragó, and C. J. Foot, Phys. Rev. Lett. **88**, 010405 (2002).

[70] J. R. Abo-Shaeer, C. Raman, J. M. Vogels, and W. Ketterle, Science **292**, 476 (2001).

[71] M. Nakahara, T. Isoshima, K. Machida, S.-I. Ogawa, and T. Ohmi, Physica B **284–288**, 17 (2000).

[72] T. Isoshima, M. Nakahara, T. Ohmi, and K. Machida, Phys. Rev. A **61**, 063610 (2000).

[73] A. E. Leanhardt, A. Görlitz, A. P. Chikkatur, D. Kielpinski, Y. Shin, D. E. Pritchard, and W. Ketterle, Phys. Rev. Lett. **89**, 190403 (2002).

[74] H. Pu, C. K. Law, J. H. Eberly, and N. P. Bigelow, Phys. Rev. A **59**, 1533 (1999).

[75] Y. Shin, M. Saba, M. Vengalattore, T. Pasquini, C. Sanner, A. Leanhardt, M. Prentiss, D. Pritchard, and W. Ketterle, Phys. Rev. Lett. **93**, 160406 (2004).

[76] L.-C. Crasovan, G. Molina-Terriza, J. P. Torres, L. Torner, V. M. Pérez-García, and D. Mihalache, Phys. Rev. E **66**, 36612 (2002).

[77] L.-C. Crasovan, V. Vekslerchik, V. M. Pérez-García, J. P. Torres, D. Mihalache, and L. Torner, Phys. Rev. A **68**, 63609 (2003).

[78] A. J. Leggett and F. Sols, Found. Phys. **21**, 353 (1991).

[79] A. J. Leggett, in *Bose-Einstein Condensation*, edited by A. Griffin, D. W. Snoke, and S. Stringari (Cambridge University Press, Cambridge, 1995), Chap. 19, p. 452.

[80] E. P. Gross, Nuovo Cimento **20**, 454 (1961).

[81] L. P. Pitaevskii, Zh. Éksp. Teor. Fiz. **40**, 646 (1961), [Sov. Phys. JETP **13**, 451 (1961)].

[82] A. L. Fetter and A. A. Svidzinsky, J. Phys.: Condens. Matter **13**, R135 (2001).

[83] H. Lamb, *Hydrodynamics* (Cambridge University Press, New York, 1975).

[84] R. J. Donnelly, *Quantized Vortices in Helium II* (Cambridge University Press, Cambridge, 1991).

[85] D. J. Thouless, P. Ao, and Q. Niu, Phys. Rev. Lett. **76**, 3758 (1996).

[86] E. B. Sonin, Phys. Rev. B **55**, 485 (1997).

[87] J. J. García-Ripoll and V. M. Pérez-García, SIAM Journal on Scientific Computing **23**, 1316 (2001).

[88] C. V. Ciobanu, S.-K. Yip, and T.-L. Ho, Phys. Rev. A **58**, 033607 (2000).

[89] M. Koashi and M. Ueda, Phys. Rev. Lett. **84**, 1066 (2000).

[90] T. Bergeman, D. L. Feder, N. L. Balazs, and B. I. Schneider, Phys. Rev. A **61**, 063605 (2000).

[91] C. Cohen-Tannoudji, J. Dupont-Roc, and G. Grynberg, *Atom-Photon Interactions* (Wiley, New York, 1992).

[92] J. F. Dobson, Phys. Rev. Lett. **73**, 2244 (1994).

[93] A. L. Fetter and D. Rokhsar, Phys. Rev. A **57**, 1191 (1998).

[94] W. Kohn, Phys. Rev. **123**, 1242 (1961).

[95] L. P. Pitaevskii and A. Rosch, Phys. Rev. A **55**, R853 (1997).

Abstracts of Publications I–V

I. It has been shown that a vortex in a Bose-Einstein condensate with spin degrees of freedom can be created by manipulating with external magnetic fields. In the previous work [Phys. Rev. A **61**, 063610 (2000)] an optical plug along the vortex axis has been introduced to avoid Majorana flips, which take place when the external magnetic field vanishes along the vortex axis while it is created. In the present work, in contrast, we study the same scenario without introducing the optical plug. The magnetic field vanishes only in the center of the vortex at a certain moment of the evolution and hence we expect that the system will lose only a fraction of the atoms by Majorana flips even in the absence of an optical plug. Our conjecture is justified by numerically solving the Gross-Pitaevskii equation, where the full spinor degrees of freedom of the order parameter are properly taken into account. A significant simplification of the experimental realization of the scenario is attained by the omission of the optical plug.

II. It is shown that a vortex can be continuously created in a Bose-Einstein condensate with hyperfine spin $F = 2$ in a Ioffe-Pritchard trap by reversing the axial magnetic field adiabatically. It may be speculated that the condensate cannot be confined in the trap since the weak-field seeking state makes transitions to the neutral and the strong-field seeking states due to the degeneracy of these states along the vortex axis when the axial field vanishes. We have solved the Gross-Pitaevskii equation numerically with given external magnetic fields to show that this is not the case. It is shown that a considerable fraction of the condensate remains in the trap even when the axial field is reversed rather slowly. This scenario is also analysed in the presence of an optical plug along the vortex axis. Then the condensate remains within the $F_z = 2$ manifold, with respect to the local magnetic field, throughout the formation of a vortex and hence the loss of atoms does not take place.

III. The stability of doubly quantized vortices in dilute Bose-Einstein condensates of ^{23}Na is examined at zero temperature. The eigenmode spectrum of the Bogoliubov equations for a harmonically trapped cigar-shaped condensate is computed and it is found that the doubly quantized vortex is spectrally unstable towards division into two singly quantized vortices. By numerically solving the full three-dimensional time-dependent Gross-Pitaevskii equation, it is found that the two singly quantized vortices intertwine before decaying. This work provides an interpretation of recent experiments [A. E. Leanhardt et al., Phys. Rev. Lett. **89**, 190403 (2002)].

IV. We investigate the recently found stationary vortex cluster states in dilute atomic Bose-Einstein condensates confined by a nonrotating trap, and also present a new stationary three vortex cluster. We find the stationary states by minimizing directly an error norm for the stationary Gross-Pitaevskii equation, and study the

dynamic and energetic stability of the resulting states by solving the corresponding Bogoliubov equations for the elementary excitations. The results are verified by integrating the time-dependent Gross-Pitaevskii equation. Contrary to previously reported results, the stationary states were observed to be both energetically and dynamically unstable. The dynamical decay rate of the clusters is typically very slow, but it should be experimentally observable. The most promising circumstances to experimentally generate and observe these structures and their dynamics is in weakly dissipative condensate systems, using phase-imprinting techniques.

V. We study the energies and decay of elementary excitations in weakly interacting Bose-Einstein condensates within a finite temperature gapless second order theory. The energy shifts for the high-lying collective modes turn out to be systematically negative compared with the Hartree-Fock-Bogoliubov-Popov approximation and the decay of the low-lying modes are found to exhibit collapse and revival effects. In addition, perturbation theory is used to qualitatively explain the experimentally observed Beliaev decay process of the scissors mode.